AD NUMBER

AD831742

LIMITATION CHANGES

TO:

Approved for public release; distribution is unlimited. Document partially illegible.

FROM:

Distribution authorized to U.S. Gov't. agencies and their contractors; Critical Technology; JAN 1968. Other requests shall be referred to Air Force Rome Air Development Center, EMATE, Griffiss AFB, NY. Document partially illegible. This document contains export-controlled technical data.

AUTHORITY

radc, usaf ltr, 17 sep 1971

DEVELOPMENT OF A C-BAND PHASED ARRAY CROSSED-FIELD AMPLIFIER

A. Wilczek

S-F-D Laboratories, Incorporated

This research was supported by the Advanced Research Projects Agency of the Department of Defense and was monitored by Capt. DuBois, RADC (EMATE), GAFB, N.Y. 13440 under Contract No. AF30(602)-4082.

FOREWORD

This Final Technical Documentary Report covers the work performed under Contract AF 30(602)-4082, ARPA Order No. 136, Amendment No. 11, from 1 March 1966 to 31 October 1967. It is published for information only and does not necessarily represent the recommendations, conclusions or approval of the Air Force.

This contract with S-F-D laboratories, Inc., Union, New Jersey, was sponsored by the Advanced Research Projects Agency under the technical direction of the Rome Air Development Center, Air Force Systems Command, Griffiss Air Force Base, New York. Capt. R. DuBois was the technical monitor for the program.

The work was performed by the Crossed-field Amplifier Department of S-F-D Laboratories. R. A. La Plante, Manager of the Crossed-field Amplifier Department, was the project manager. Technical supervision was performed by F. A. Feulner, Technical Manager of the Crossed-field Amplifier Department. The electrical performance evaluation was conducted by A. Wilczek, Project Engineer.

ABSTRACT

The purpose of this effort was to conduct a C-band phased array crossed-field amplifier program to deliver a tube capable of supplying 1 megavatt of peak power with an average power output of 10 kilowatts across a 500 MHz band centered at 5.65 GHz. The amplifier, which is dc operated with control electrode turn off, is to be packaged in a 10 inch diameter magnetically shielded package with integral permanent magnets.

The design and development of this tube were directly based upon results which were obtained on a program conducted under Contract AF 30(602)-3633. A particularly significant result of the program under that contract was the development of a new slow wave structure for broad band forward wave amplifiers. This new structure, the helix coupled vane (HCV) circuit has demonstrated bandwidths in excess of the present requirements. Matching studies on the HCV circuit have resulted in a very good match over approximately 1 GHz.

A cathode material study was initiated, in which several materials were examined for their suitability for use in the high power dc operated amplifier. Of the several materials examined, an impregnated tungsten matrix type produced the best results and was subsequently used.

Dc operation on a vehicle in an electromagnet showed nearly full instantaneous bandwidth at peak power levels of 700 to 805 kilowatts at a pulse length of approximately 32 μsec. This vehicle was subsequently operated at 5.9 GHz and generated 1 megavatt peak power and 10 kilowatts of average power.

Phase measurements were performed on three vehicles in the program.

TABLE OF CONTENTS

LIST OF ILLUSTRATIONS

1.0 INTRODUCTION

The purpose of this program was to conduct a C-band phased array crossed-field amplifier program to deliver a tube to the specifications of Exhibit "A" of the program contract, which are summarized in Figure 1. The tube is a broad band, high peak and average power output C-band amplifier, which is to be dc operated with control electrode turn off. In addition, the amplifier is to be packaged in a 10" diameter magnetically shielded permanent magnet package.

The principle of dc operation and control electrode turn off was first demonstrated at L-band on a 100 kw peak power output tube (SFD-209), developed under Contract AF 30(602)-2533. It has since been extended to tubes operating at UHF, S-, C-, and X-band.

The design and development of this tube are more directly based upon the results which were obtained on a program conducted under Contract AF 30(602)-3633, where an X-band 100 kw peak power output, broad band dc operated tube was developed. A particularly significant result of the X-band work was the development of a new slow wave structure for broad band forward wave amplifiers. This new structure, the helix coupled vane (HCV) circuit, has demonstrated bandwidths in excess of the present 10% requirements.

A cathode material study program was initiated, in which several materials were examined for their suitability for use in the dc operated amplifier. The material studies were conducted in a test vehicle which reproduced the current density and peak power objectives of this program. Tests on an impregnated tungsten matrix showed this cathode material to be capable of operating at the megawatt peak power level and at several kilowatts of average power with stable operation.

Matching studies on the HCV circuit have resulted in a very good match over approximately 1000 MHz. Two versions of the HCV circuit have been studied in cold test and are identified as Type A and Type B circuits. The vehicles withstood the dc breakdown test, which

Center frequency	5.65 GHz
Instantaneous bandwidth (1 db)	500 MHz
Peak power output	1 Mw
Average power output	10 kw
Gain	13 db
Cathode voltage	-75 kv max
Control electrode Mu	3 minimum
Efficiency	
Minimum	40%
Average	50%

FIGURE 1 TARGET PERFORMANCE SPECIFICATION FOR C-BAND PHASED ARRAY CROSSED-FIELD AMPLIFIER

requires a maximum hold off of 35 kv and a hold off of 32 kv for a period of at least 30 minutes.

Dc operation measurements on one vehicle in an electromagnet showed nearly full instantaneous bandwidth at peak power levels of 700 kw to 850 kw and average powers of 2.0 kw to 2.5 kw at a pulse length of approximately 32 μsec. This vehicle was subsequently operated at 5.9 GHz in an electromagnet and generated 1 Mw peak power and 10 kw average power.

The magnetic circuit employed in the final design is a magnetically shielded package where there is little or no external field developed, so that tubes may be stacked in close proximity to each other or to other magnetic materials. The circuit consists of permanent magnets placed on top and bottom of the amplifier and the circuit is enclosed by a soft iron return shell.

A magnetically shielded amplifier was completed but was capable of only modest power output (200 kw to 300 kw peak). Indications were that the cathode was improperly positioned in the interaction space and a correction could not be made on the tube before the program funds were expended. The tube nevertheless verified the magnetic circuit design.

Phase measurements were performed on three vehicles in the program. These results are presented in the performance section.

2.0 DESCRIPTION

The type of amplifier selected for this task is described as a reentrant stream forward wave amplifier in a circular format which utilizes a drift space between the input and output waveguide terminals. The reentrant electron stream leads to operation at high peak power with high efficiency, and the drift space between input and output serves the purpose of removing the RF information from the reentering electron stream. A schematic of this device is shown in Figure 2. It consists essentially of a cylindrical slow wave circuit surrounding a circular cathode

The RF drive power is introduced through a ceramic vacuum window into ridged waveguide which couples the energy via impedance transformers to the slow wave circuit. As the wave travels along the slow wave circuit, it extracts energy from a rotating electron cloud which moves in synchronism with the phase velocity of the wave on the slow wave circuit. The amplifier signal is extracted in the same way through ridged waveguide and is passed through the output vacuum window.

The slow wave circuit used is known as a helix coupled vane (HCV) circuit. The circuit consists of a number of active sections where amplification takes place, and a number of non-propagating sections in a drift space where demodulation or debunching of the reentrant electron stream takes place. The drift space also provides RF isolation between the input and output terminals of the slow wave circuit.

The control electrode is mounted on the cathode assembly and is located in the drift space. The control electrode is pulsed positive with respect to the cathode after the input signal is removed and collects the reentering space charge to terminal amplification.

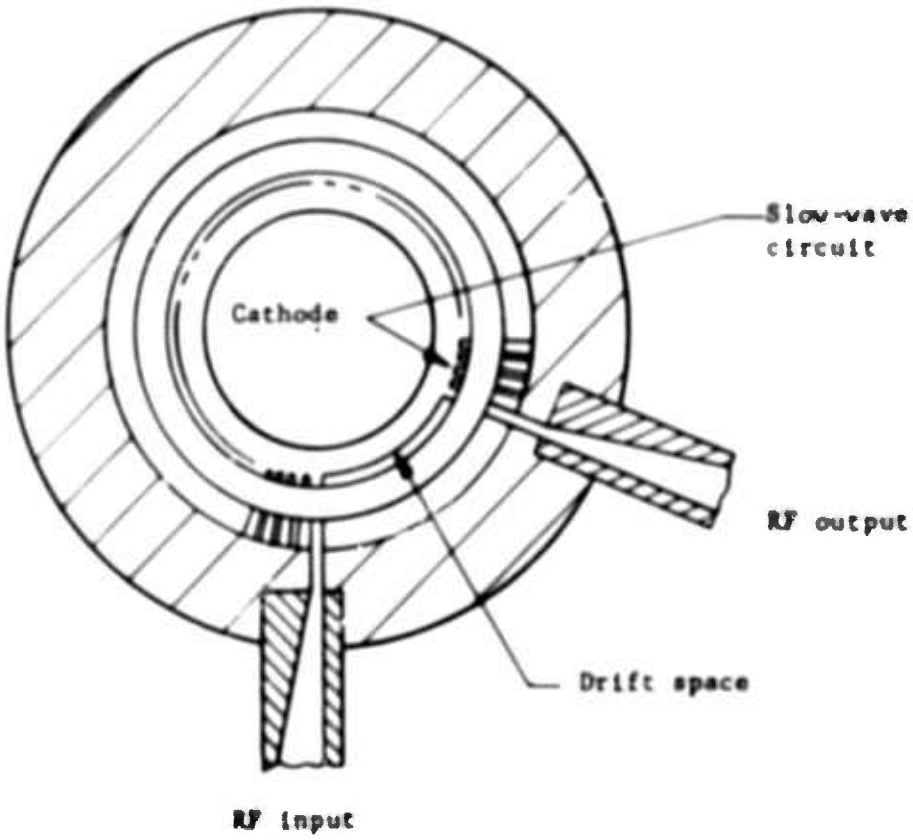

FIGURE 2 SCHEMATIC DIAGRAM OF AN S-F-D LABORATORIES CROSSED-FIELD AMPLIFIER

3.0 TUBE DESIGN

The following sections set forth the order of the design procedure. Parameters such as operating voltage and current, bandwidth, efficiency, size and weight were examined theoretically in some length to explore tradeoffs in the design. Having fixed the critical dimensions of the interaction structure, a complete mechanical design layout was made. Following this, the study of the properties of the slow wave circuit via cold tests could begin.

3.1 The Slow Wave Circuit

From the operating parameters such as voltage, current, power output, frequency, bandwidth, gain and efficiency, a model was established for the dispersion characteristic which would be required to realize such performance. Analyses of the HCV circuit were made to establish critical dimensions such as circuit pitch, circuit length, and cathode diameter, and to select the size and shape of the helices and vanes. From these analyses, models of the circuit can be made to confirm or correct the dimensions selected by means of cold tests.

The cold test work involved the design and evaluation of two versions (Type A and Type B) of the HCV circuit. The general configuration of the circuit, shown in Figure 3, is that of a series of vanes coupled electrically by a pair of rectangular helices, one on each side of the vane. Electronic interaction occurs between the cathode and the vane. The design of these circuits is based upon the performance obtained on the X-band HCV circuit under Contract AF 30(602)-3633. The C-band circuits have been scaled down in frequency and up in peak power and will provide the necessary anode area for average power dissipation.

The dispersion curves for the Type A and Type B HCV circuits were measured on linear models. A typical linear model of the HCV circuit used on the program is shown in Figure 4. The two dispersion curves are shown in Figure 5. It can be seen that the Type B circuit model has a "flatter" dispersion (was more dispersive) than the Type A circuit model. Both models had adequate bandwidth to meet the operating bandwidth requirements.

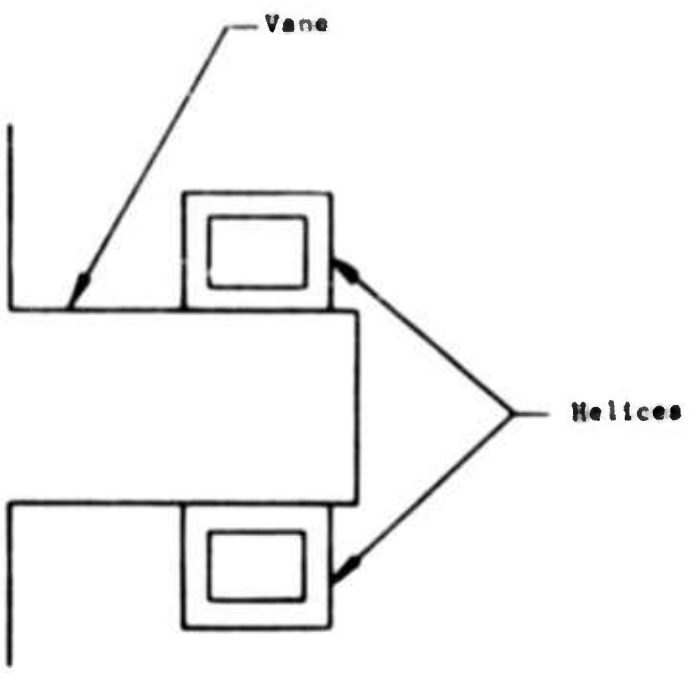

FIGURE 3 SCHEMATIC OF HCV CIRCUIT

The parallel helices are used for symmetry

FIGURE 4 LINEAR MCV CIRCUIT TESTER

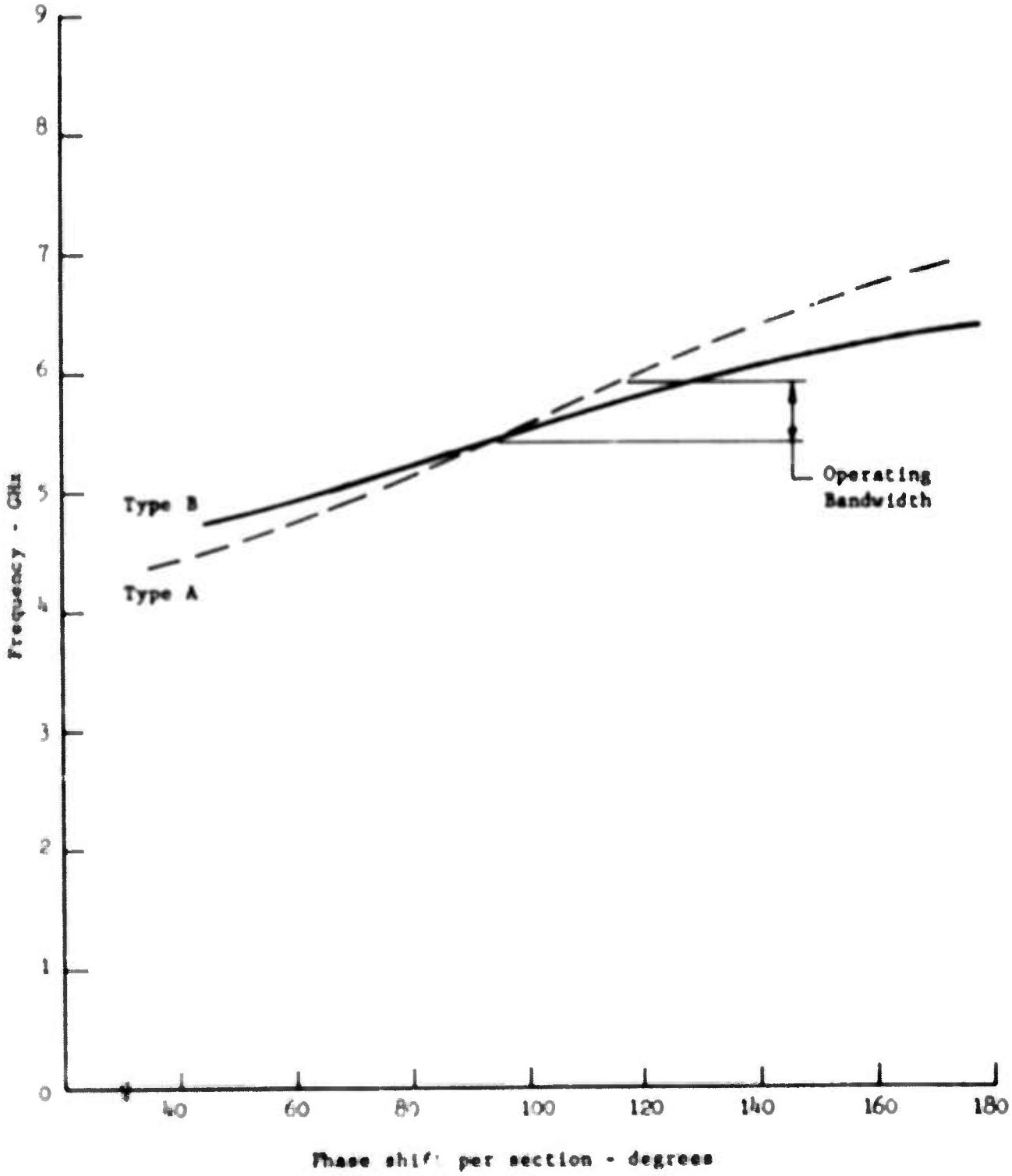

FIGURE 5 DISPERSION CURVES FOR TYPE A AND TYPE B HCV CIRCUITS

Circular cold test models of both circuits were then built to further confirm their dispersion and interaction impedance characteristics. A photograph of a circular cold test model is shown in Figure 6. The input and output coupling ports can be seen on either side of the solid drift space portion of the circuit. The dispersion curves were as predicted by the linear models. Interaction impedance measurements were made on both HCV circuits. These measurements were made using dielectric perturbation of the electric fields. The results show that the interaction impedance of the Type B circuit is higher than that of the Type A circuit. A part of this increase in impedance is due to the "flatter" dispersion curve of the Type B circuit. The interaction impedance of a circuit is inversely proportional to its group velocity and the group velocity is given by the slope of the dispersion curve. A more significant portion of the increased impedance is due to the different distribution of RF energy on the Type B circuit resulting from its dimensional configuration.

3.2 Impedance Matching

Cold test work was successful in establishing that the dispersion curve of the circuit models was correct as far as could be determined prior to the evaluation of the circuit on hot test. Since our plan was to incorporate the Type A circuit into the first vehicle scheduled for hot test, the matching effort on that circuit was given priority. The selection of the Type A circuit was based upon its being less dispersive than the Type B circuit and its interaction impedance was believed to be adequate for our goals.

The first hot test vehicle, designated G25H, was assembled before matching studies had been completed in order to make a preliminary evaluation of the electronic design of the amplifier. The circuit match for G25H is shown in Figure 7 and shows that the circuit is useable only over the lower portion of the required operating band. Improvements were made in the circuit match following the construction of G25H.

The improved Type A circuit match yielded a return loss curve shown in Figure 8. The measurement shows the combined reflection from both input and output circuit matches. These data show an average return loss of approximately 15 db over more than 1000 MHz. This type of match characteristic was felt to be quite satisfactory. These

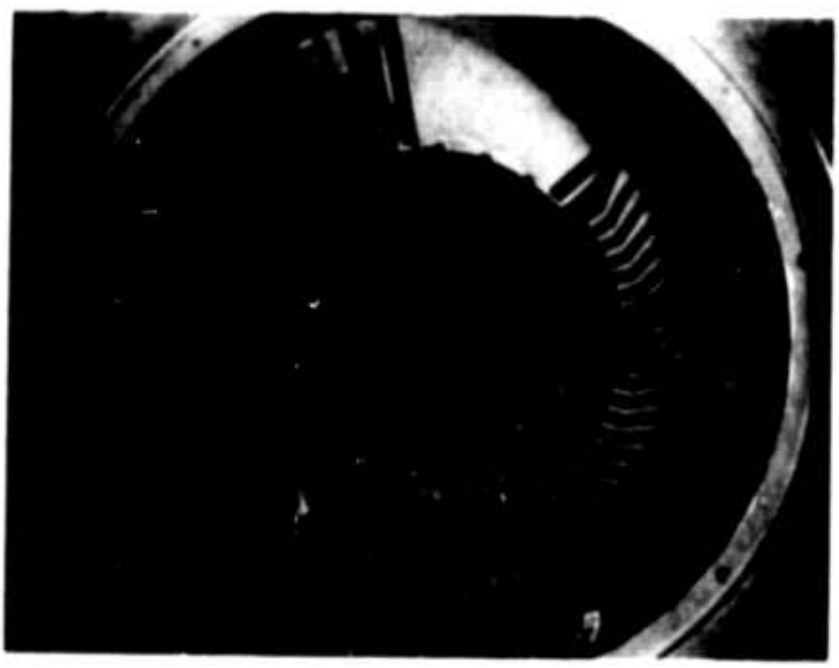

FIGURE 6 CIRCULAR HCV CIRCUIT

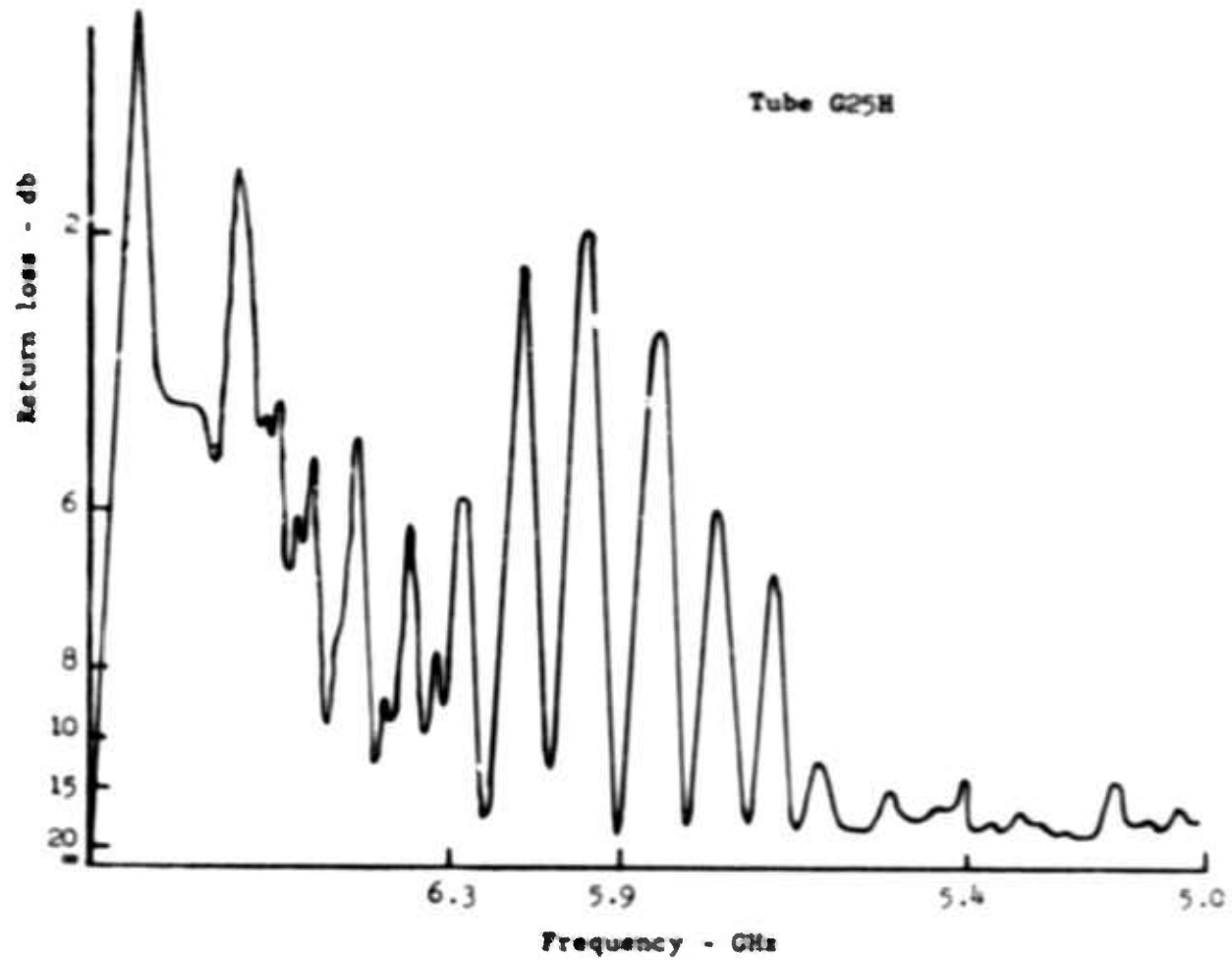

FIGURE 7 MATCH OBTAINED FOR FIRST HOT TEST VEHICLE, TUBE G25H

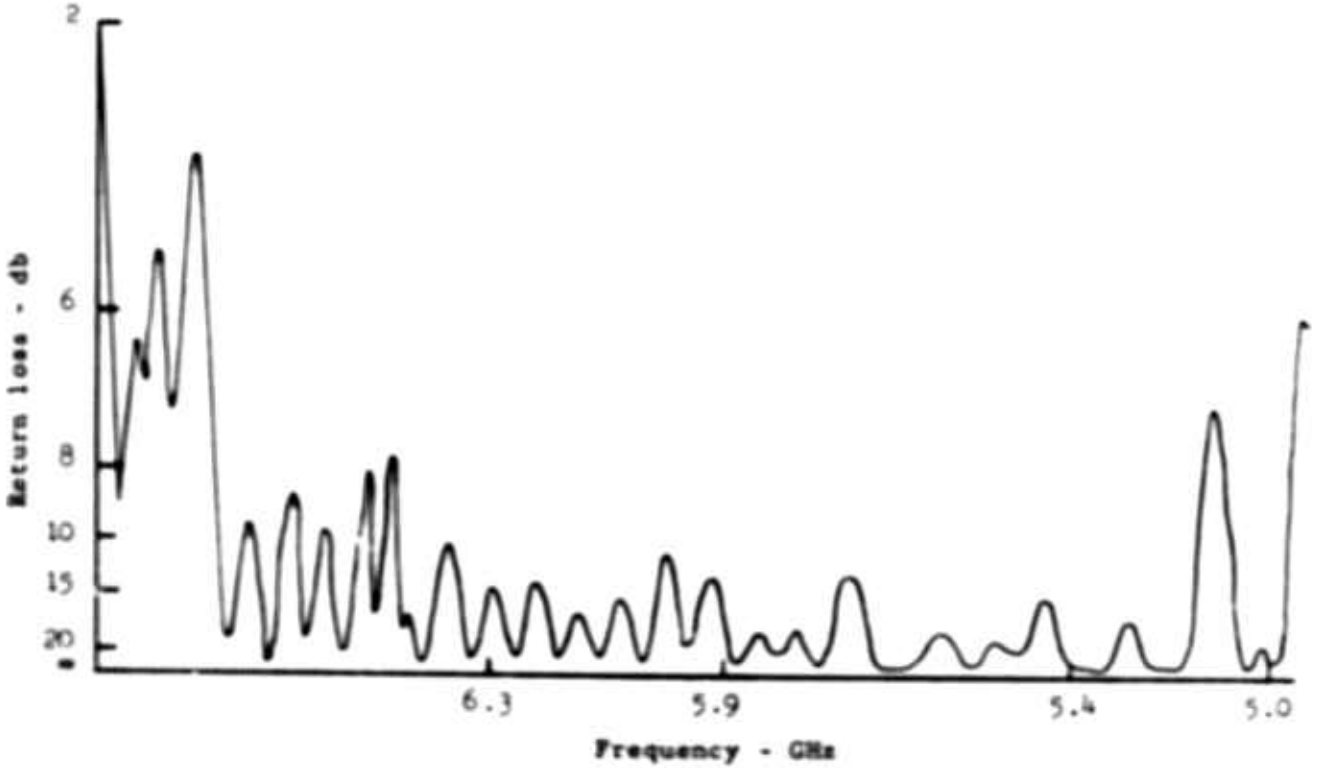

FIGURE 8 IMPROVED MATCH OF TYPE A CIRCUIT FOR USE IN SECOND HOT TEST VEHICLE

results, coupled with acceptable hot test results subsequently obtained with the Type A circuit, led to the termination of matching efforts with the Type B circuit.

The second test vehicle, designated I32H, was built incorporating the improved match. The return loss results were similar to those shown in Figure 8, i.e., an average return loss of 15 db over approximately a 1.2 GHz band. These data also show mismatch contributions of both input and output and include the effects of a full length circuit.

The third test vehicle, designated J35H, was built by an outside vendor with the intention of developing another source for the anodes. The vendor's inexperience in this type of work resulted in an anode that was not structurally perfect. The overall result was a match that was considered useable but slightly inferior in comparison to the other vehicles. The match is shown in Figure 9. The first hot test vehicle, G25H, was rebuilt to incorporate the improved match and the return loss results are shown in Figure 10.

The final design hot test vehicle, G15I, was built with input and output waveguides bent to permit them to be enclosed by the magnetic circuit. Initial match results for this vehicle are shown in Figure 11. Later match data obtained on the vehicle just prior to hot test and shown in Figure 12 are poorer than the initial results. We suspect that the circuit may have been slightly damaged during assembly, since normal handling does not produce such pronounced changes in the match.

3.3 Cathode Material Studies

A program was initiated in which several materials were examined for their suitability for use in the dc operated high power crossed-field amplifier. A number of studies have been made in the past to examine materials for their secondary emission properties. However, it is felt that the results obtained are only useful in cataloging these materials. Experience has shown that the results obtained from carefully controlled secondary emission tests do not

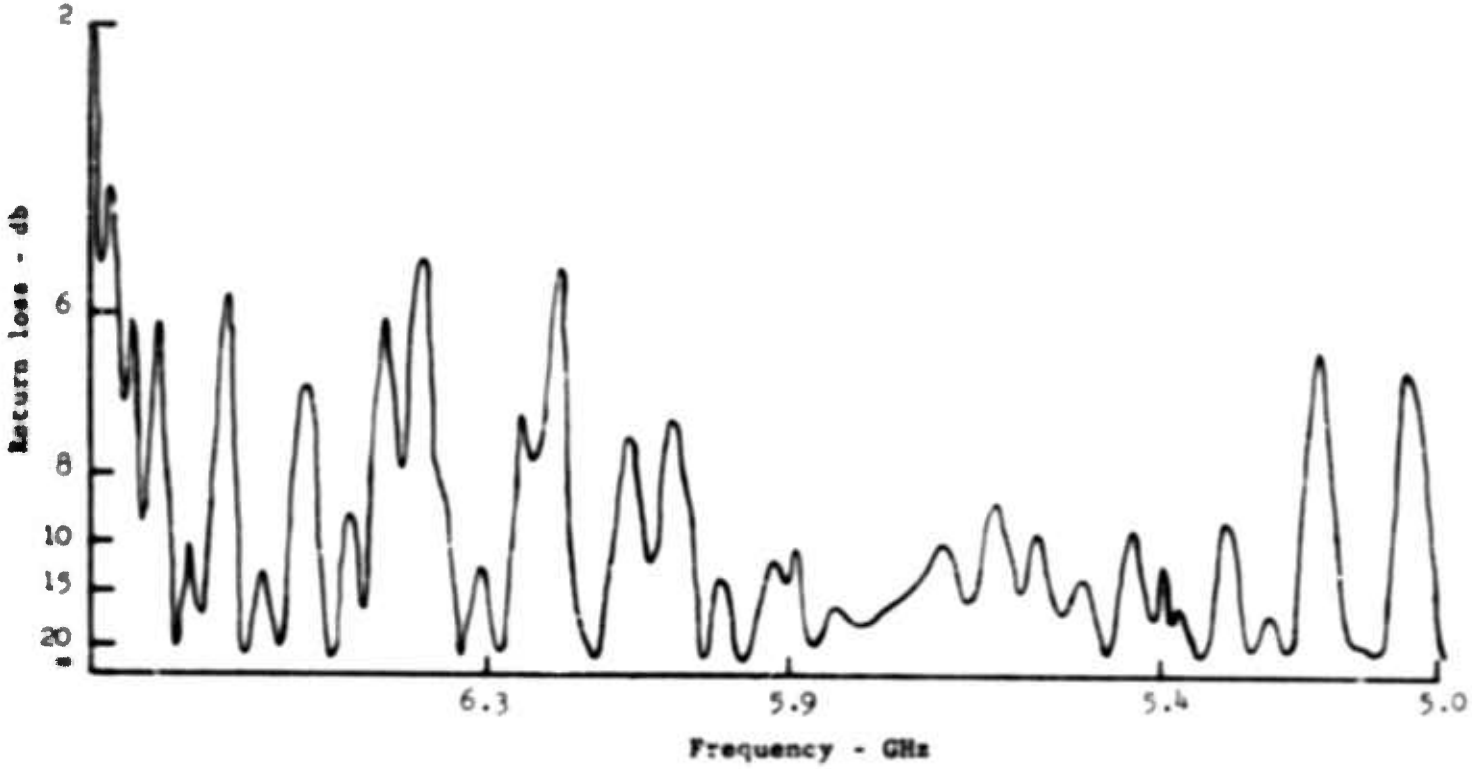

FIGURE 9 INPUT MATCH FOR HOT TEST VEHICLE J35N AFTER BAKEOUT

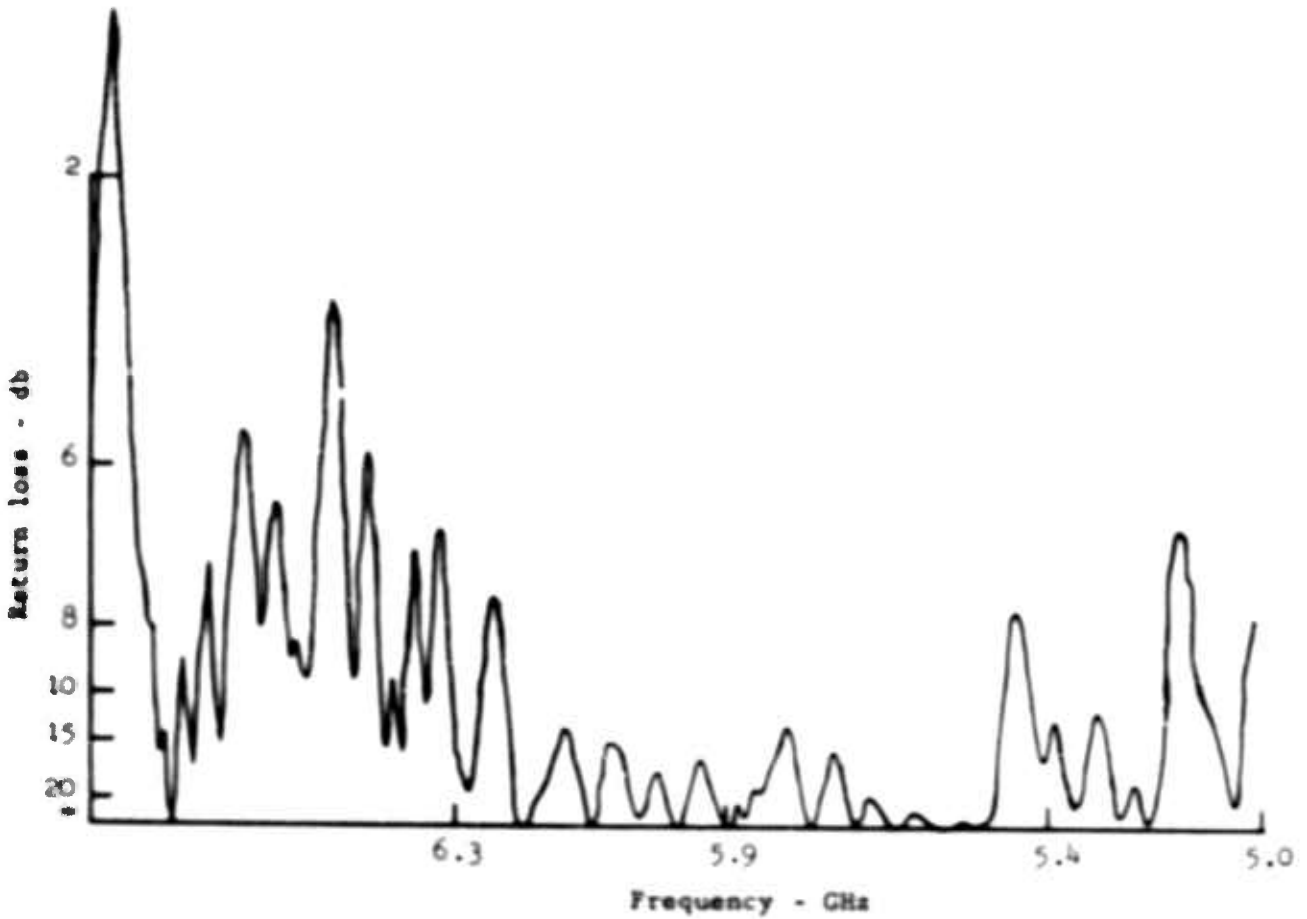

FIGURE 10 IMPROVED MATCH OF FIRST HOT TEST VEHICLE, G25H

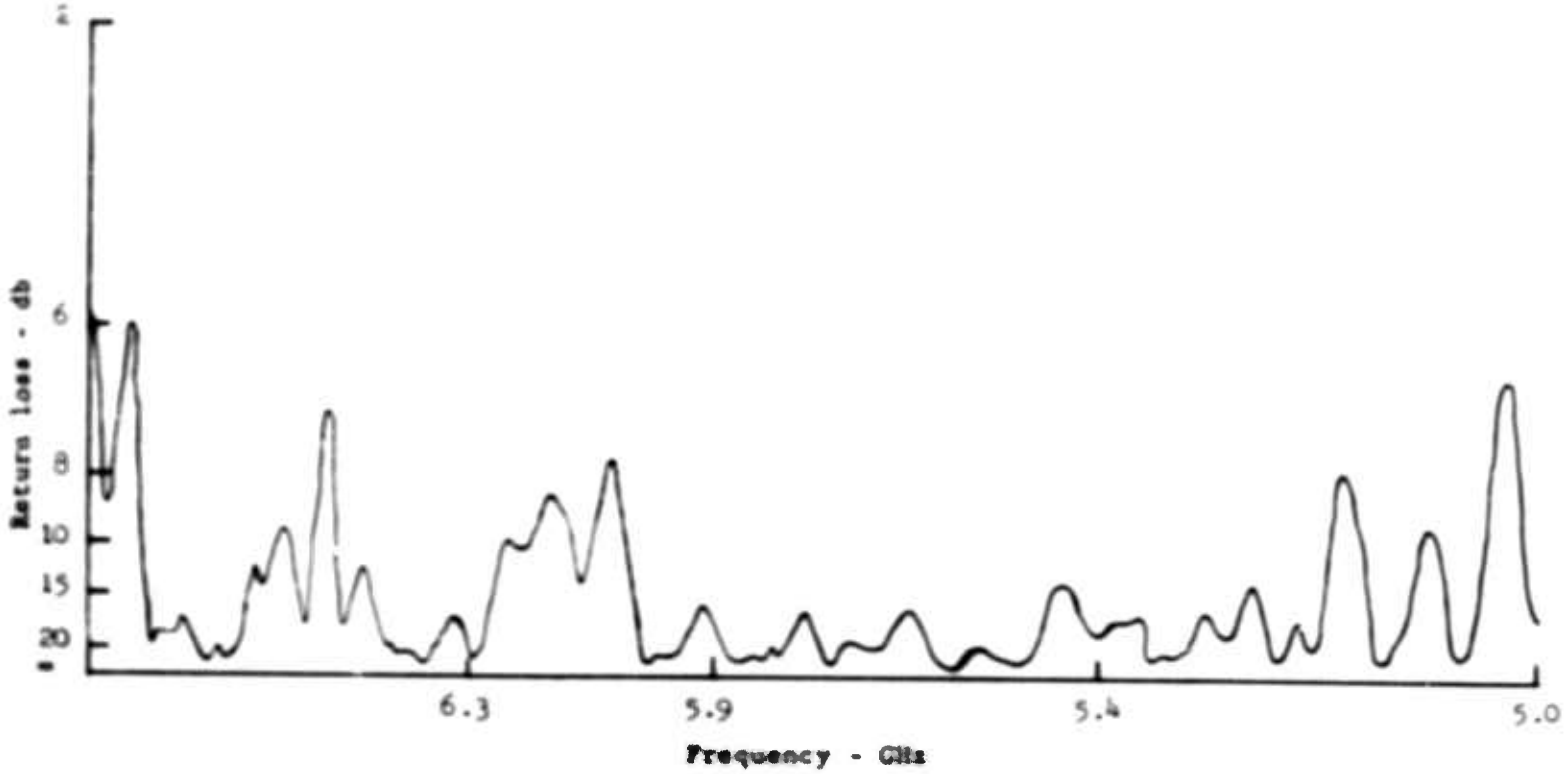

FIGURE 11 INITIAL MATCH FOR FINAL DESIGN VEHICLE, G151

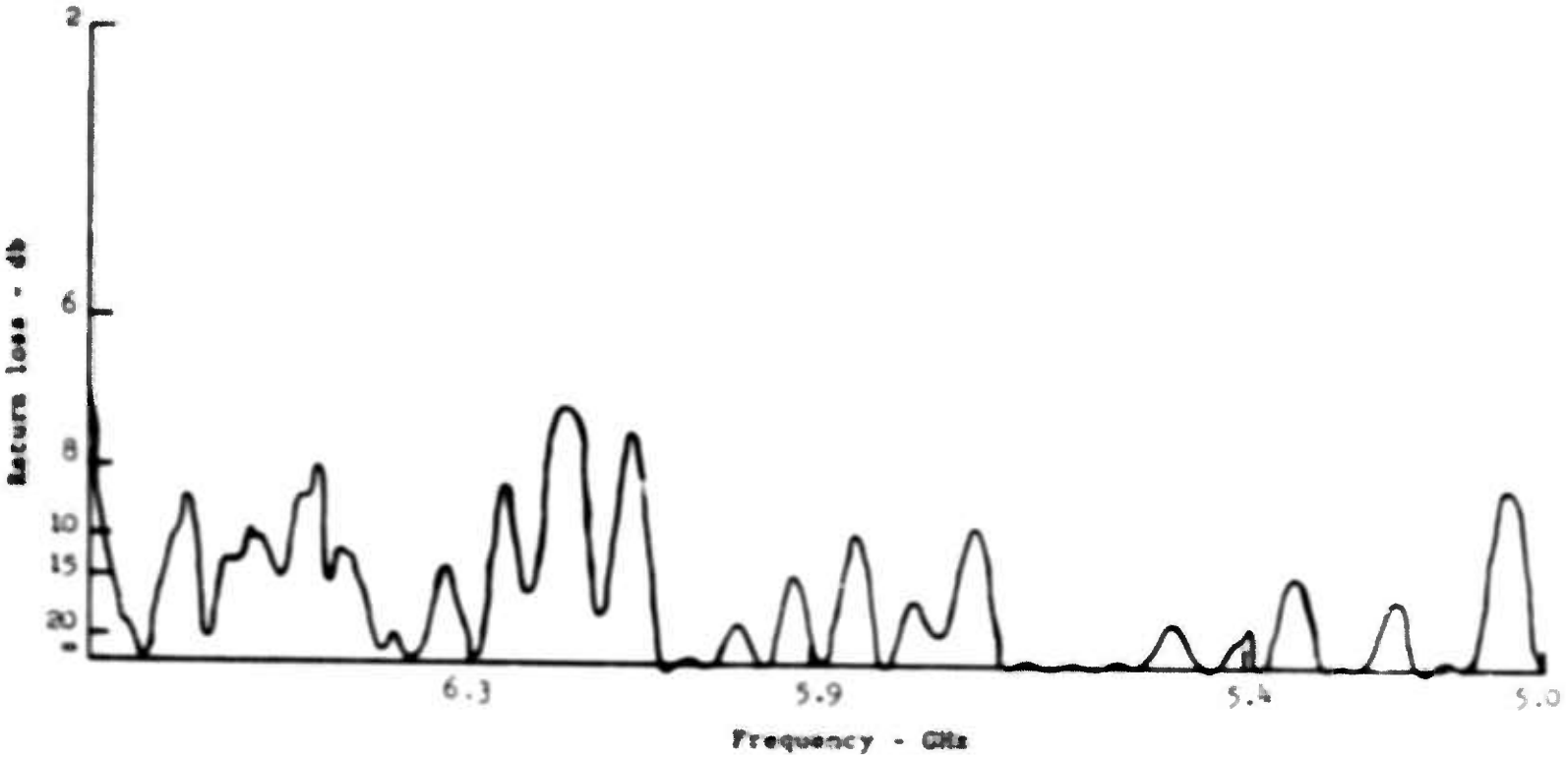

FIGURE 12 MATCH OF G151 AFTER ASSEMBLY

necessarily indicate how the material will behave in the actual operating environment of a crossed-field amplifier. It was felt necessary that the materials to be investigated be studied in an environment which duplicates the conditions expected in the final design. The final amplifier design must be capable of operation at high peak and high average power simultaneously during a relatively long pulse.

To obtain such information on cathode materials, a program was planned which utilizes a high power backward wave amplifier as the test vehicle. The vehicle used was the SFD-231 C-band amplifier which operates with a 30 μsec pulse and delivers peak powers in excess of 1 Mw with average powers in excess of 3.5 kw. The test vehicle was rebuilt several times so that the materials investigated were tested and compared with the least number of variables.

It should be pointed out that a cathode material that is suitable for operation in a cathode pulsed tube is not necessarily usable in an RF pulsed tube (which has a dc voltage applied), because the latter cannot operate satisfactorily if the cathode emits thermionically. The cathode material suitable for use in a high power crossed-field amplifier utilizing dc operation should ideally have the following characteristics:

1. A relatively high secondary emission ratio (δ) at low back bombardment energy levels for ease of starting; should be high enough so that starting delays do not exceed two or three electron transits around the tube;

2. the second unity crossover of the secondary emission characteristic should occur at relatively high back bombardment energy levels for high peak power operation;

3. the surface of the secondary emitting material should be stable and insensitive to breakdown during electron bombardment;

4. the thermionic emission from the cathode during the interpulse period should be minimum even at slightly elevated temperature.

The test procedure was designed to indicate the limits on amplifier operation imposed by the cathode material. The procedure was to first evaluate the maximum current boundary during high power operation at full pulse width at three frequencies covering the band of operation. The cathode material was then further evaluated by operation at high peak power and low average power, while keeping the cathode temperature very low. Observations have indicated that under this type of operating condition the cathode surface can readily be stripped of emitting material or may be contaminated. With thoriated tungsten or barium impregnated cathodes, the emitting material on the surface can be replenished by operation at elevated temperature. However, the high temperature also produces thermionic emission which cannot be tolerated.

One material tested was a tungsten matrix impregnated with a barium compound. This material is used where primary emission must be a minimum. The initial results indicated that this material was capable of supplying the necessary cathode current at full operating conditions with cathode temperature maintained at less than 300°C. The vehicle was operated at peak powers well in excess of 1 Mw at average power output in excess of 5.5 kw with a 27 μsec pulse length. The cathode did not exhibit any instabilities after it had aged during the first half hour of operation. The life capability test did not indicate any changes in emission under the most severe operating conditions. Past experience had shown that some forms of barium impregnated cathodes fail after only one or two hours of operation under these conditions. The tests were sufficiently informative to suggest the use of this material in the first hot test vehicle. A continuation of evaluations in the SFD-231 was therefore felt to be of limited value. The cathode material studies would, of course, be resumed if tests on the program's dc operated amplifiers indicated any serious cathode deficiencies.

3.4 Cooling

Three elements of the amplifier require cooling: the anode (slow wave circuit), the cathode, and the output ceramic window. The anode and output window can be cooled in a relatively straightforward manner. The cathode, which operates at high voltage, requires additional consideration in its cooling because the cooling specification requires that the coolant be at ground potential and that there be one input and one output coolant connection. This is accomplished by using a high resistivity coolant and a closed loop recirculating system with a heat exchanger. The input and output coolant connections are at ground potential.

The input water enters the package at ground potential and goes to the output window. The water leaves the output window and is connected to the cathode through insulated tubing long enough to provide insulation from the cathode potential with a minimum of leakage current through the tubing and the column of coolant. The coolant then comes in direct contact with the control electrode and cathode to provide for efficient heat transfer and greater thermal capabilities. The coolant leaves the cathode assembly through another insulated tubing, similar to that entering the cathode, and enters the anode block. The coolant, now at ground potential, leaves the anode block and emerges from the package.

A flow rate of 2.5 gal/min at 35 psi pressure drop was adequate for the amplifier and held the bulk temperature rise of the coolant to approximately 30°C at the 10 kw average power output level.

3.5 Magnetic Circuit

The program requires that the tube delivered be packaged in a 9" maximum diameter shielded structure. The basic package design is shown in Figure 13.

The magnets used in this type of configuration are cylindrical and abut the amplifier body itself on each side. The return path for

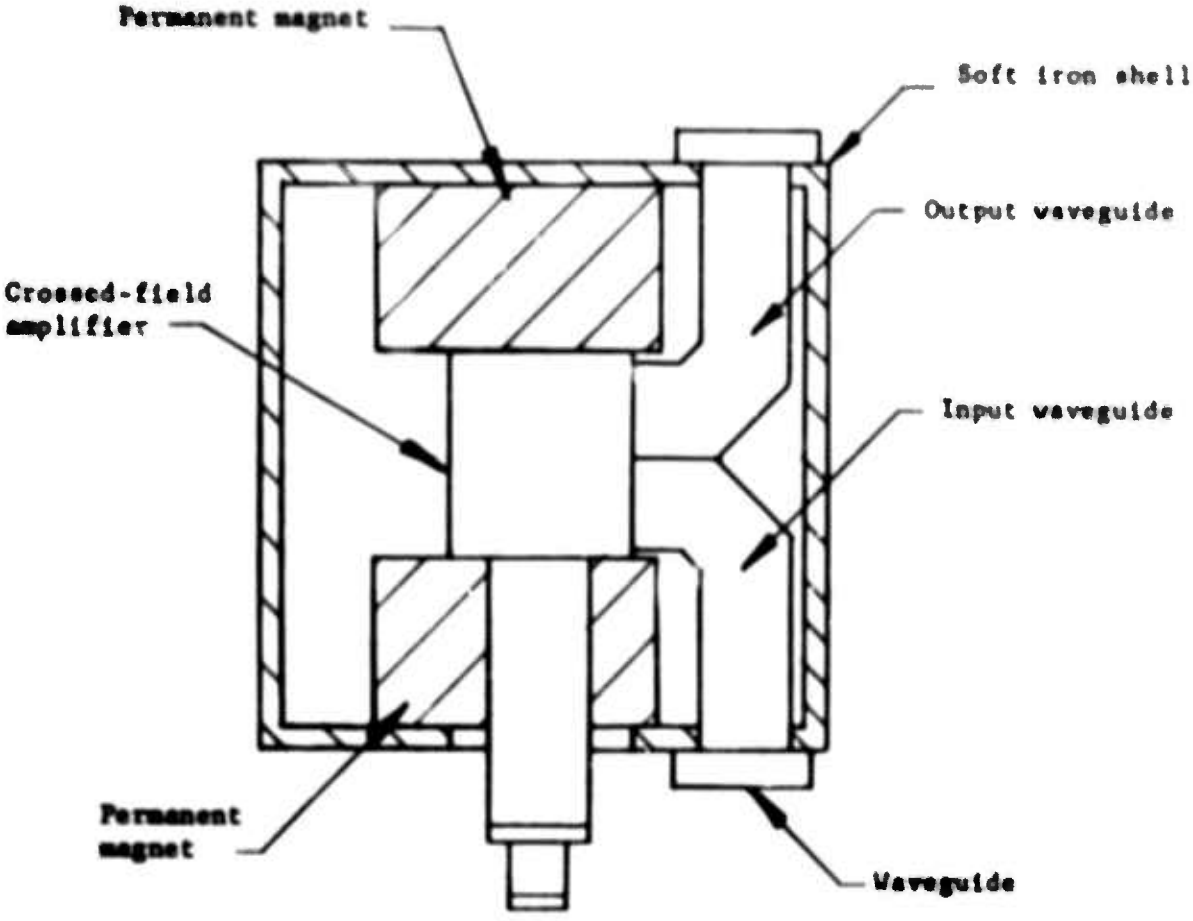

FIGURE 13 CUT-AWAY SKETCH OF SHIELDED CROSSED-FIELD AMPLIFIER PACKAGE

the flux is provided by means of a soft iron shell which surrounds the entire assembly. The design of the magnet and shielding shell is such that leakage flux adjacent to the shielding shell is small enough to permit amplifiers to be operated adjacent to each other without causing mutual interference.

To evaluate various magnetic geometries, a magnetic cold tester was designed. The magnetic material planned for the package is Alnico V-7. This magnetic material was chosen as one which has sufficient coercive force and flux density capability to drive the air gap required while at the same time will be quite readily available from more than one supplier.

The first test structure resulted in a package which was 9" in diameter and approximately 21" long, and is shown in Figure 14. The particular magnets chosen were adequate to provide the required flux density in the gap, but at the same time were not adequate to supply the leakage flux to the shielding shell which resulted from the geometry chosen. This leakage flux caused the magnet material to work at a higher flux density than anticipated and resulted in a lower coercive force with which to drive the gap. This, in turn, resulted in a lower magnet field in the gap than was required.

After extensive effort to raise the field level in the gap was not successful, the only alternative left was a larger diameter shell, i.e., a 10" outer diameter shell, in order to reduce the amount of leakage flux and permit the magnets to operate with a higher coercive force.

The larger diameter shell was evaluated and the required field was obtained. The magnetic field in the gap is 4200 gauss to 4300 gauss.

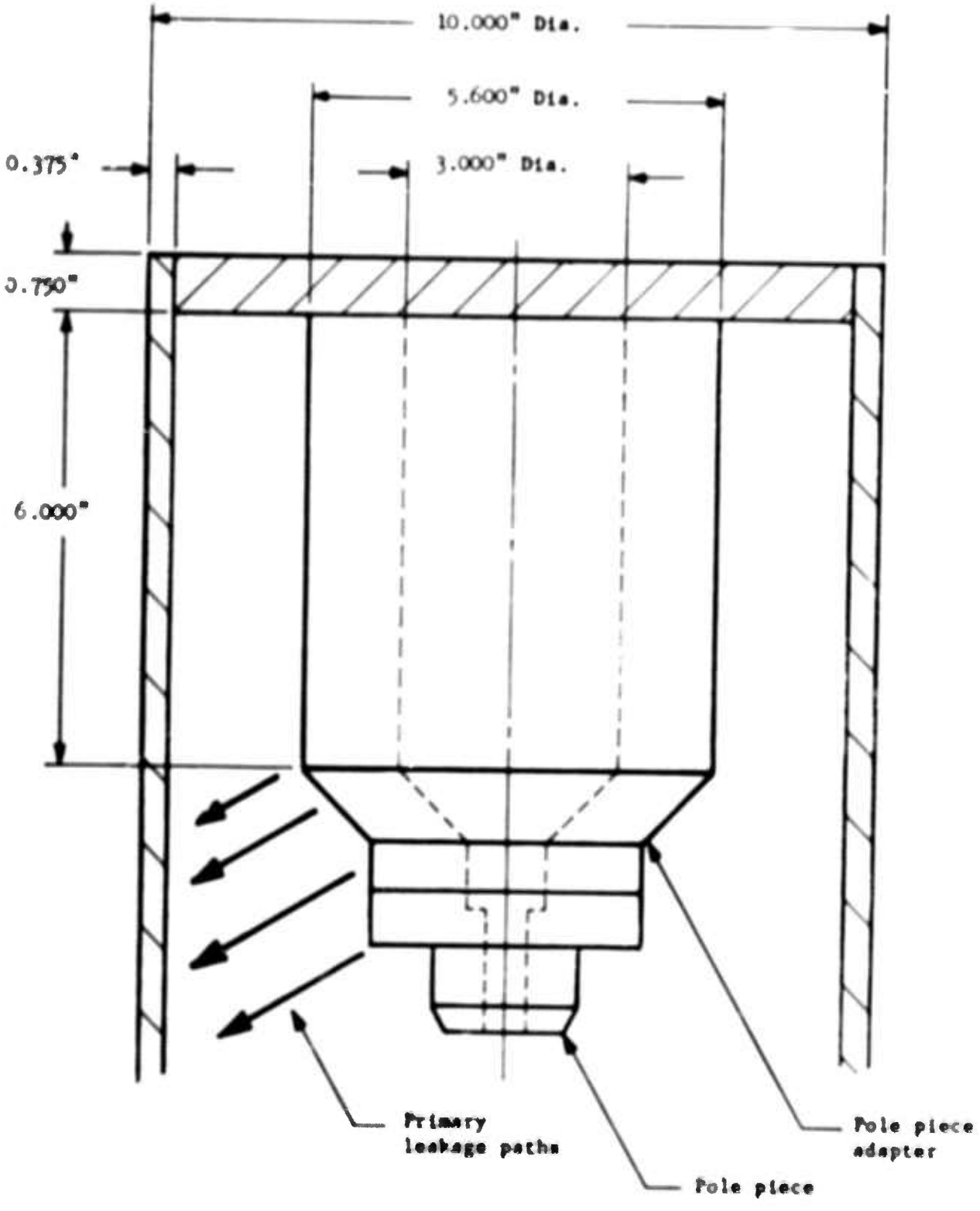

FIGURE 14 DRAWING OF MAGNETIC TEST STRUCTURE

3.6 Phase Measurements

The phase measurements were made using a null detection method shown schematically in Figure 15. The measurement begins by balancing the phase bridge (adjusting it for a null) using the precision attenuator (H) and the phase shifter (G). The null is observed on an oscilloscope which displays detected power output of the bridge as a function of time for the pulse length of interest. This initial balance is obtained with the amplifier operating under a prescribed set of conditions. The measurement proceeds by tuning the tube (changing the RF drive frequency) across the operating band in a sufficient number of frequency increments to insure the desired accuracy. The amount of phase shift for each increment is read directly from the phase shifter after each null is obtained. The precision attenuators which are set initially to balance the "T" need not be changed after the initial setting since the small amplitude variations observed over the band do not upset the accuracy of the measurement.

The components of the phase bridge are carefully selected (that is, high directivity directional couplers, low VSWR attenuators, etc.) to reduce the possibility of other measurement errors.

Normally, the deviation from linearity is obtained by plotting the measured phase versus frequency characteristic, by drawing the best straight line through the points, and by observing the peak deviations which occur. The use of a straight line as a reference from which to observe the deviations is valid for only certain conditions. Because of the measuring system used here and the relatively large bandwidth over which the measurement is made, an allowance must be made for curvature in the dispersion characteristics of the waveguide.

Curvature due to the dispersion characteristic of the waveguide can be avoided by inserting equal lengths of waveguide in both arms of the bridge. To do so would result in a very high rate of change of phase versus frequency in the output of the bridge because

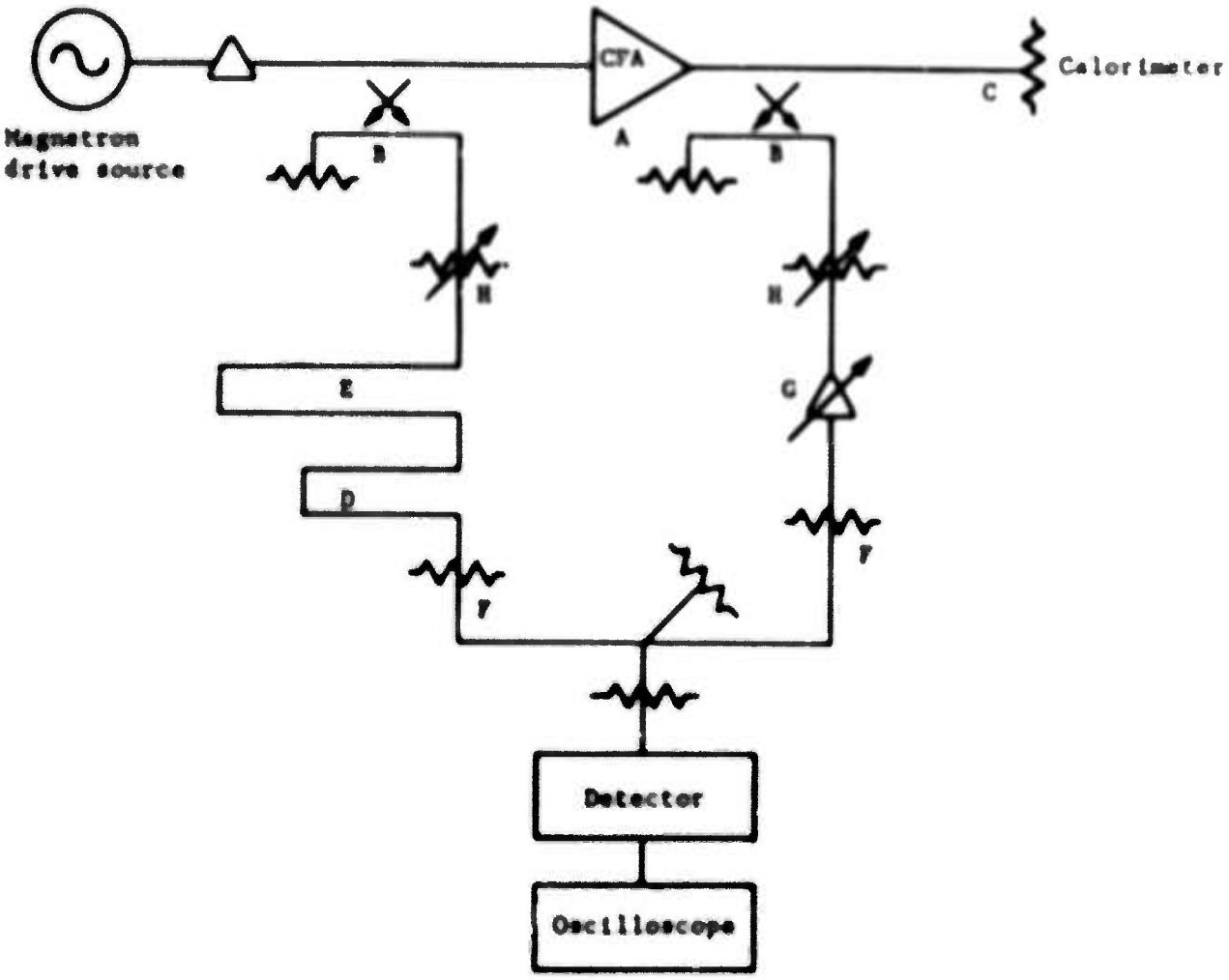

A Crossed-field amplifier
B 40 db directional coupler
C High power water load
D Compensating length of J-band waveguide
E Compensating length of C-band waveguide
F Fixed attenuator
G J-band precision phase shifter
H Precision attenuator

FIGURE 15 SCHEMATIC OF PHASE BRIDGE

the electrical length of the amplifier under test makes one of the bridge arms much longer than the other. This was felt to be a problem since frequency increments would have to be chosen such that the incremental phase shift would be less than 180° to avoid ambiguity in the phase shifter readout. In addition, the total variation in phase reading from one end of the band to the other would amount to approximately 1600° and this would prevent a straightforward display of data. One could, of course, subtract a straight line function from the measured results to compensate for this. The method chosen is described below.

A length of waveguide is added to the input arm of the bridge such that its length and dispersion will create for the input arm approximately the same rate of change of phase with frequency as the amplifier, with its electrical length and dispersion, would produce in the output arm of the bridge. This leads to our having unequal amounts of waveguide in the arms of the bridge. If one assumed that the amplifier on test were perfectly linear, the output of the bridge arranged in this way would not be a straight line, but would have curvature caused by the waveguide dispersion characteristic. The peak deviation of this curved standard has been calculated to be approximately 6° from a straight line.

Additional contribution to curvature was previously encountered. It was caused by the use of some waveguide components in one arm of the bridge (precision attenuators and phase shifter) made with smaller sized waveguide which is more dispersive in the frequency region in which it was being used than normal C-band waveguide. This was subsequently corrected by adding equal lengths of the same type of waveguide to the other bridge arm. We feel the only contributor to curvature now is the difference in length of C-band waveguide in each arm.

The measured data are then compared with the curved standard of the bridge. The results plotted as deviations from the linearity are shown for three vehicles in Figures 16, 17, and 18. Both operating

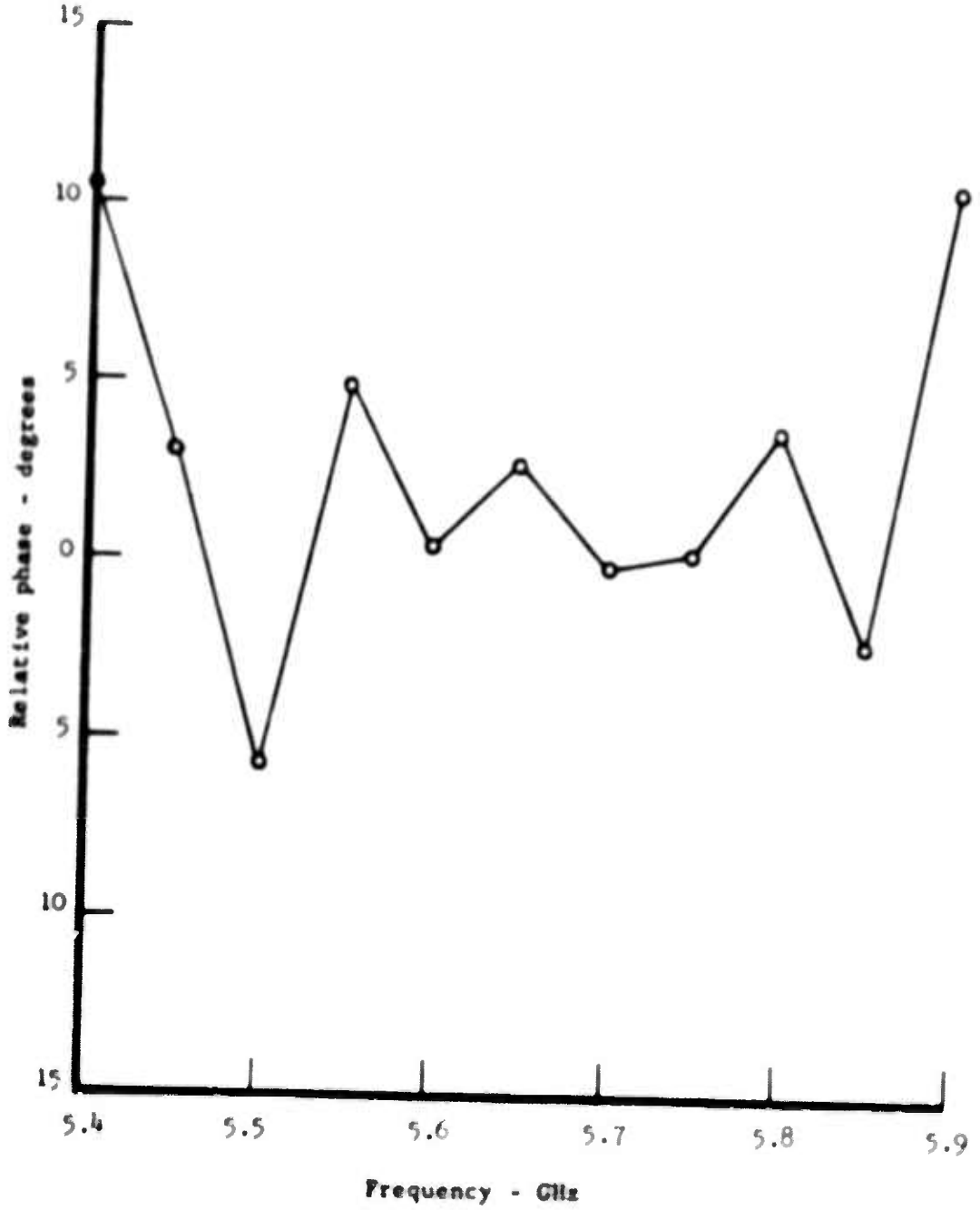

FIGURE 16 DEVIATION FROM LINEARITY, TUBE G25H-6

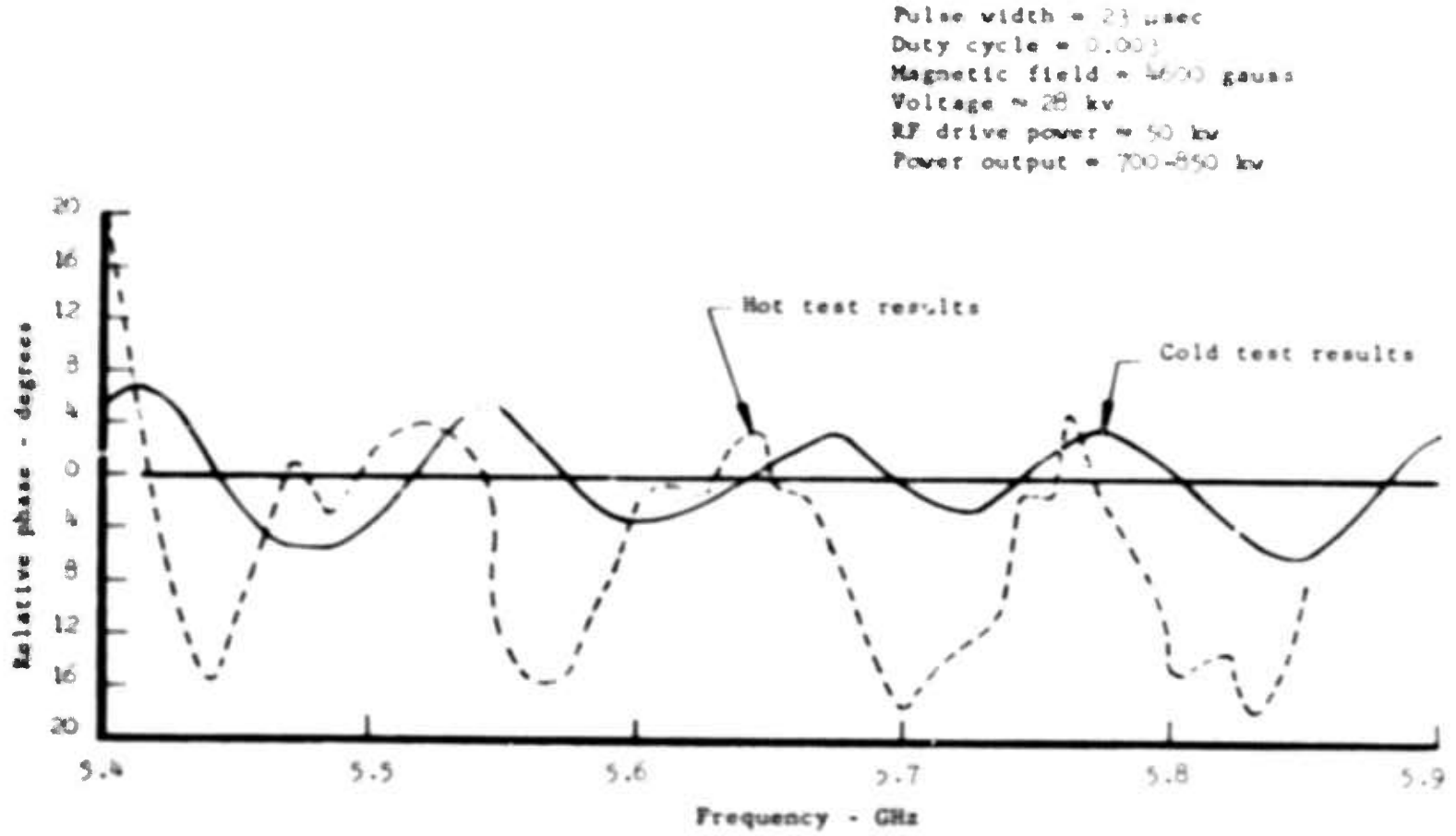

FIGURE 17 DEVIATION FROM LINEARITY, TUBE 1328-2

Pulse width = 23 μsec
Duty cycle = 0.005
Anode voltage = 26.5 kv
RF drive power = 25 kw
Power output = 300-400 kw

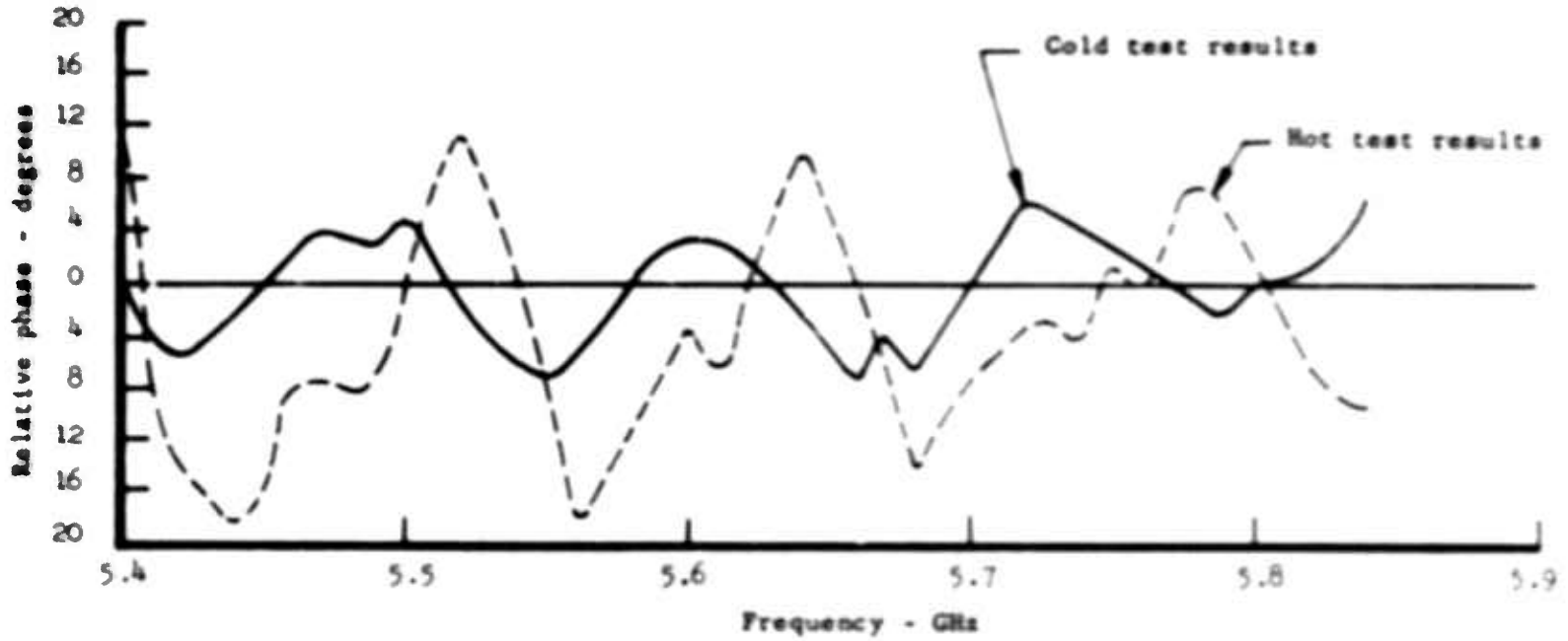

FIGURE 18 DEVIATION FROM LINEARITY, TUBE J358-1

and non-operating phase data are shown in the figures.

The data reveal a distinct periodicity. The periodicity could arise from three possible sources in the amplifier:

(1) multiple reflections caused by circuit mismatches;

(2) electronic feedback from output to input through the drift region; or

(3) RF feedback from output to input because of RF circuit coupling through the drift space.

Multiple reflections from circuit mismatches would produce a periodicity in the measured data corresponding with the frequency interval required to change the electrical length of the amplifier by 180°. Electronic feedback and RF feedback would produce the periodicity corresponding with the frequency interval required to change the electrical length of the tube by 360°. Circuit mismatch effects, therefore, would produce twice the number of ripples over the frequency band as would electronic or RF feedback. The periodicity measured corresponds with either electronic or RF feedback. Some fine structure appears on these data which we believe is related to circuit mismatch effects.

The ripple in the data is believed to be RF feedback and not electronic feedback from the following argument: the periodicity is first of all observed on a non-operating tube. If, from these data, one calculated the circuit insertion loss of the drift space, one can predict the effects of RF feedback in an operating tube according to its level of gain. Such a calculation was made and a subsequent experiment confirmed that the amplitude of the ripple observed was a function of the gain at which the amplifier operated and that there was a reasonable agreement between predicted and measured levels. We would have expected, if both RF and electronic feedback were present, to be able to account in this way for only a portion of the amplitude of the ripple. Our calculations now account for nearly all of the amplitude of the ripple, and we therefore believe the effect to be one of RF feedback.

The prediction of RF feedback effects is shown in Figure 19. If we add to a vector representing the RF input voltage to the amplifier another vector representing RF feedback, we can construct a vector diagram as shown in the figure. The amplitude of the added vector is a function of K, the gain of the amplifier, and α, the isolation or attenuation of the drift section from output to input. For fixed gain and isolation, the phase of the added vector with respect to the RF input voltage will change continuously with frequency so that the added vector will appear to rotate about the tip of the RF voltage vector. The maximum phase deviation produced can be obtained directly as

$$\theta = \sin^{-1} \alpha K$$

If we assume that the ripple is caused by RF feedback, we obtain θ and K from measurements on a non-operating amplifier (in which there cannot be electronic feedback effects) and calculate α. By then assigning to K values which it will have during operation, we can predict what the effect should be in an operating amplifier (K for a non-operating amplifier is the insertion loss of the amplifier).

The deviations measured on the vehicles agreed closely with this theory. As a result of our measurements, it appears clear that further effort is required to increase the circuit isolation between output and input through the drift space. This may be done by physically altering the match sections to the amplifier to reduce their coupling to the drift region and/or by introducing additional loss in the drift section.

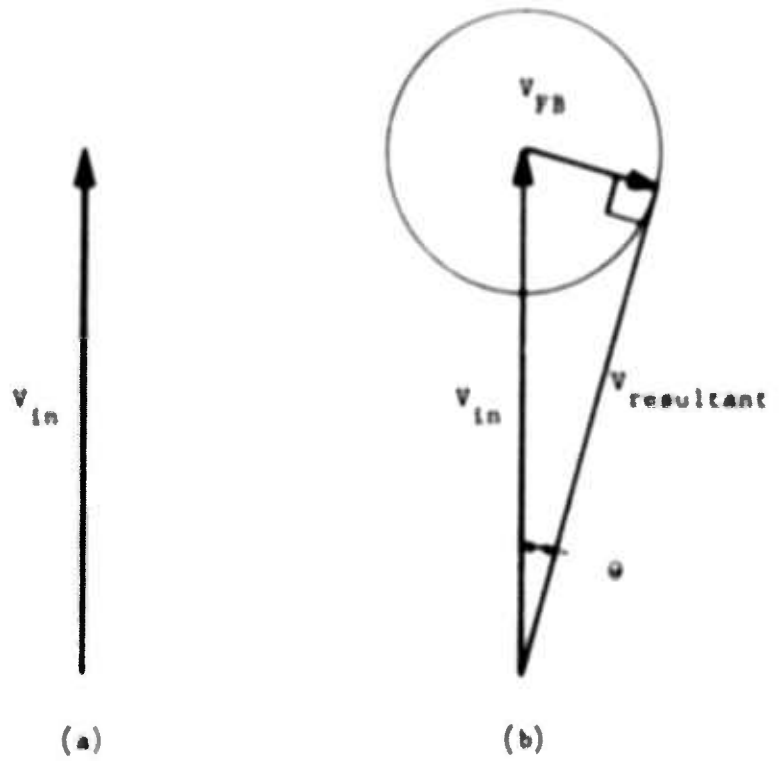

V_{FB} = voltage feedback through drift section

= $\alpha K V_{in}$

α = isolation of drift section from output to input

K = gain of amplifier

θ = phase deviation = $\sin^{-1} \alpha K$

FIGURE 19 AMPLITUDE OF PHASE DEVIATION VECTOR DIAGRAM

4.0 PERFORMANCE

The first SFD-237 vehicles to undergo hot test were made with a mechanical design which, with one exception, permits it to be used directly in the shielded permanent magnet assembly. The one exception is that the input and output waveguides were left emerging radially from the tube, whereas in the final package design the waveguides were bent along the cathode axis to emerge axially from the package.

Test procedures for the SFD-237 were developed and are described in Appendix I.

The first test vehicle utilized a Type A slow wave circuit. Both anode and cathode assemblies were liquid cooled, as was the output ceramic window. No control electrode was employed since only pulse modulated tests were planned for this vehicle. Tests conducted on the first vehicle used a line type pulsed modulator.

The tests on the first vehicle, designated G25H, showed that the tube drew current at a low voltage. This voltage was too low for the magnetic field intensity used, and it was found to be caused by operation in a band edge oscillation. Efforts to obtain signal amplification were not successful because of the band edge oscillation and no other RF duty could be obtained.

The tube was rebuilt and designated G25H-1. A change in the end hat geometry was made in an attempt to combat the band edge oscillation. No signal amplification could be obtained because of the band edge oscillation which was present, but the noticable effect of the change was that the amplifier would operate to higher peak current levels in the band edge before arcing out.

The amplifier was rebuilt again and was designated G25H-2 The design was modified to change the drift space geometry on the cathode subassembly in the area which would later be occupied by the control electrode in the design. For the first time it was possible to observe signal amplification, but all data which could be obtained showed the output still to be heavily contaminated by band edge interference.

The amplifier was rebuilt and designated G25H-3. The design was modified once more and the anode-cathode spacing was increased by 10%. This design change, coupled with the two others which had previously been made, had a significant effect on RF performance. For the first time, clean RF amplification was observed. The performance of this vehicle is shown in Figure 20. Amplification was obtained over approximately a 300 MHz band with constant applied pulse voltage of approximately 26 kv. Peak output power levels ranged from approximately 900 kw to 1.35 Mw. Efficiencies ranged from mid-40% to upper 50%. Operation at frequencies higher than 5.6 GHz was not possible because of the onset of band edge contamination which resulted from the in-band mismatches in the tube (see Figure 8). Data were obtained at a pulse length of 18 μsec and, in order to eliminate possible average power problems at this early stage, at a duty factor of 0.00045.

Tube G25H-3 developed a high internal gas pressure which was found not to be a leak. The tube was opened and it was confirmed that there was no leak; it was also examined and no physical damage was found. The tube was resealed and pumped as G25H-4. Before proceeding with RF operating tests, the vehicle was used to establish the dc hold off properties of the structure being used. The vehicle with full magnetic field and no RF drive power applied withstood voltages as high as 35 kv. After reaching that point, the tube was held in a non-operating condition at 32 kv for 30 minutes without arcing. This test was considered adequate to permit the present design to be used for the first control electrode test vehicle.

Tube G25H-4 was put on RF test again and data which were obtained confirmed the previously obtained data for tube G25H-3. High internal gas pressure, however, again developed and when the tube was opened for inspection, a cracked ceramic support was found on the cathode subassembly which indicated overheating.

The second test vehicle was already under construction. This vehicle incorporated a control electrode. It had a Type A slow wave

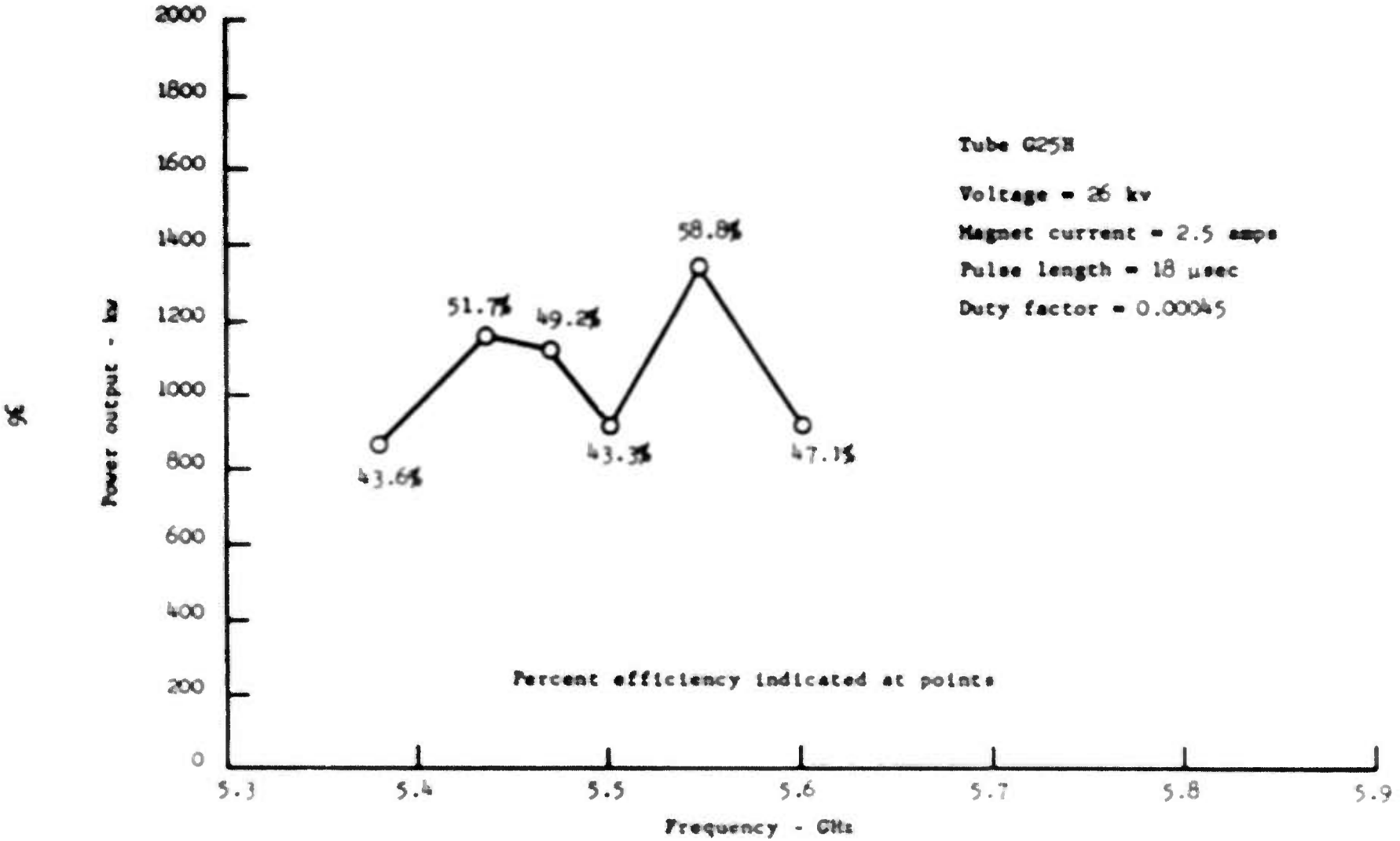

FIGURE 20 PERFORMANCE FOR TUBE G25H

circuit incorporating the match shown in Figure 8. The second test vehicle was originally to have the same type of cathode and the same cathode geometry as was used in tubes G25H-3 and G25H-4, but the evidence of the thermal inadequacies of that design and certain problems associated with the fabrication of the subassembly dictated a change in the cathode design.

Several cathode assembly design changes were carried out. These had to do mainly with the thermal capability of the structure. The control electrode portion of the subassembly has been designed so that it will function more reliably both electrically and mechanically. Improved coolant contact with both the cathode and the control electrode will account for most of the thermal capability increase of the new cathode design.

The original cathode assembly design was predicated on a desirable but not mandatory condition that cathode coolant does not contact any portion of the assembly at high potential. This resulted in a cathode design which relied upon the conduction of cathode dissipation power to the coolant through an insulating ceramic. This proved to be an undesirable and unnecessary complication. The amplifier, when contained in the system, will use a coolant which has a sufficiently high resistivity so that the packaged amplifier can be built as required with only two coolant connections, both of which will be at ground potential. The new cathode design therefore is such that the coolant is in contact with high potential internally but provision was made in the package design to incorporate the necessary insulating coolant column internal to the package.

The second test vehicle, 132H, was initially operated on the pulsed test set. The cathode and control electrode were connected externally. The tube operated at peak power levels of 200 kw to 300 kw at a duty cycle of 0.001. It was observed that the end hats were visibly hot. The vehicle was transferred to the dc test set, but no satisfactory

information was obtained. It was decided to rebuild the tube with improved end hat cooling. This was accomplished by increasing the contact area between end hats and cathode shank; i.e., lowering the thermal impedance. The tube was rebuilt as 1328-1. Operation of the tube was still not satisfactory, although some improvement was observed in end hat cooling. The improved cooling allowed tested at a duty cycle of 0.003 before the end hats became visibly hot. The low power conditions of 200 kv to 300 kv obtained were due to a peak current limit of approximately 15 amps, above which the amplifier would not operate.

The information obtained from 1328-1 was used in the design of the third test vehicle, designated 1358. With a further improvement in the end hat cooling by increasing the end hat to cathode shank contact area again, and a change in the internal geometry to provide a more uniform magnetic field, the vehicle was dc operated to peak power levels of 400 kv to 500 kv across the band with a minimum of 47% efficiency. The data are shown in Figure 21. The average power output was approximately 2.5 kw with a pulse length of 37 μsec. Phase data were also taken on the vehicle and are presented in Figure 22. The phase data yielded a deviation from linearity which was unexpectedly large. This is explained in the section on phase measurements.

Further testing at the upper end of the band produced as much as 750 kv of peak power on dc with an average power output of 4.5 kw. At this average power level, no significant gas pressure or end hat temperature was noted. The further improved end hat cooling now seems to be adequate. At this time, the energy storage capacitors broke down and further testing had to await repair.

We received a request from RADC for more detailed information concerning phase data, saturation effects, and control electrode characteristics on the SFD-237 to be submitted by 1 December 1966. Two vehicles were built in the short time allotted. These were 0258-6 and 1328-2.

	Curve A	Curve B
Anode voltage	24 kv	25 kv
Duty cycle	0.005	0.005
Cathode current	34-44 amps	32-40 amps
Pulse length	37 μsec	37 μsec
Magnet current	2.7 amps	3.0 amps

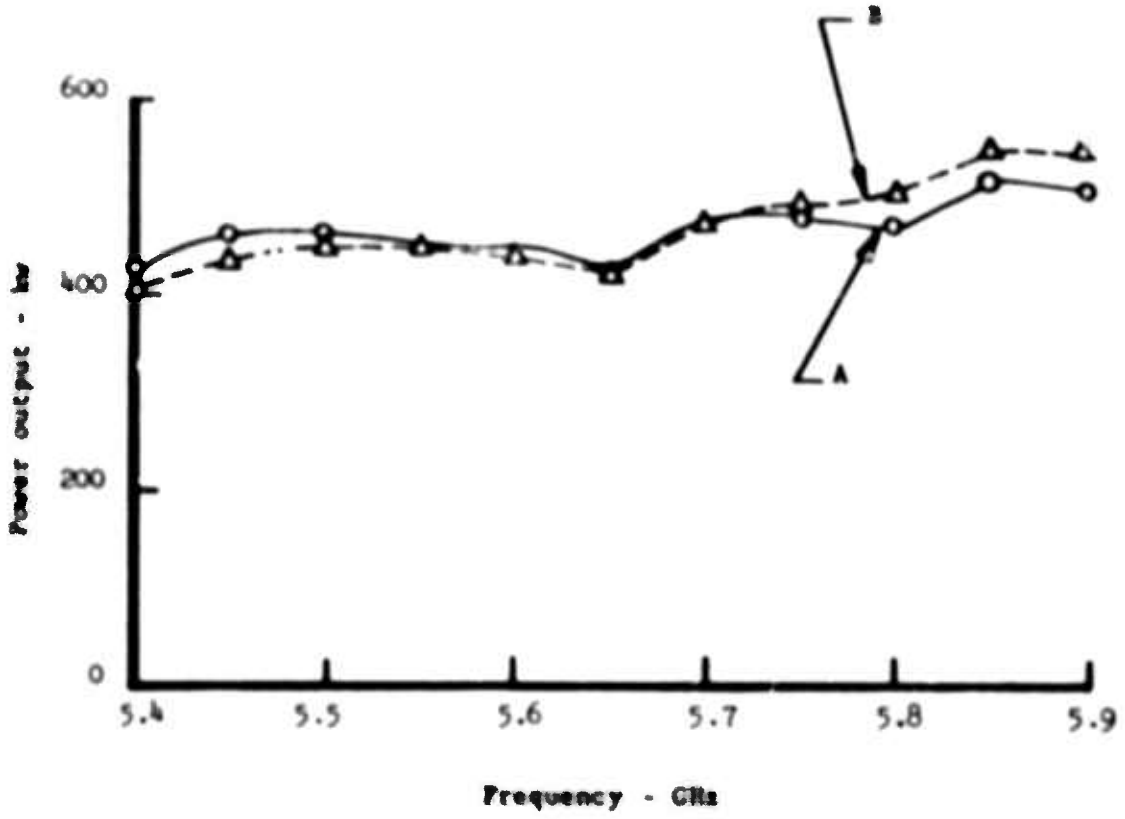

FIGURE 21 POWER OUTPUT VERSUS FREQUENCY FOR TUBE J35H

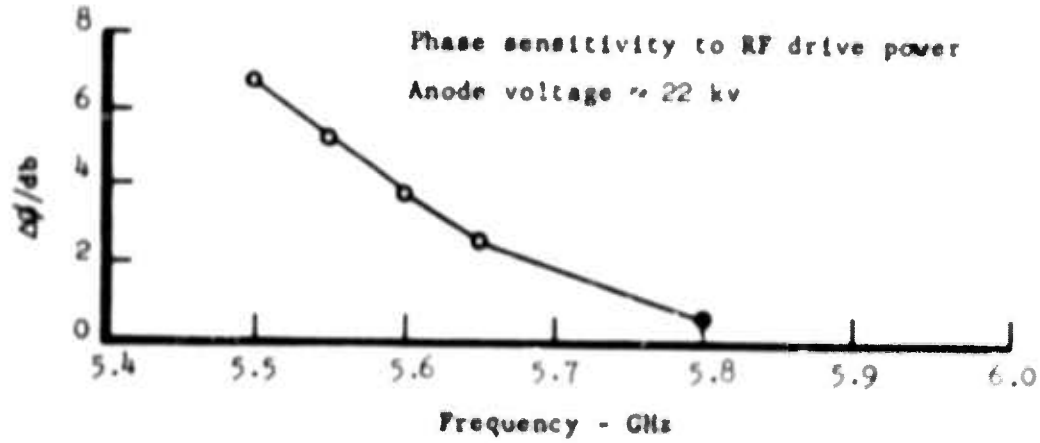

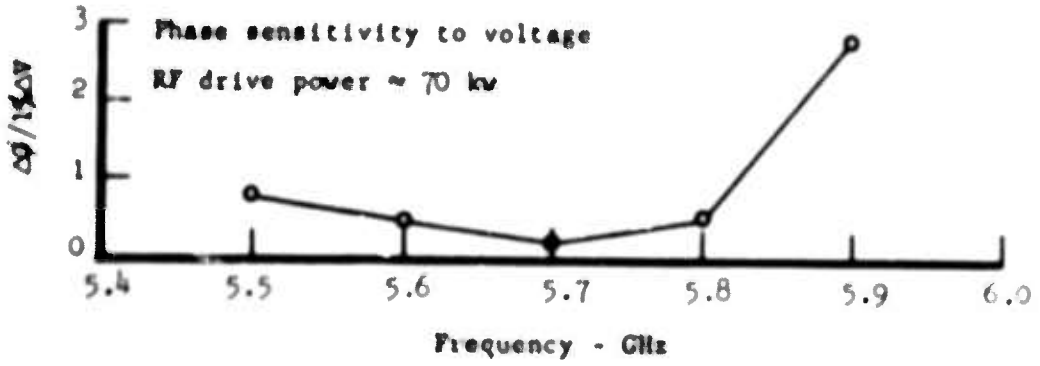

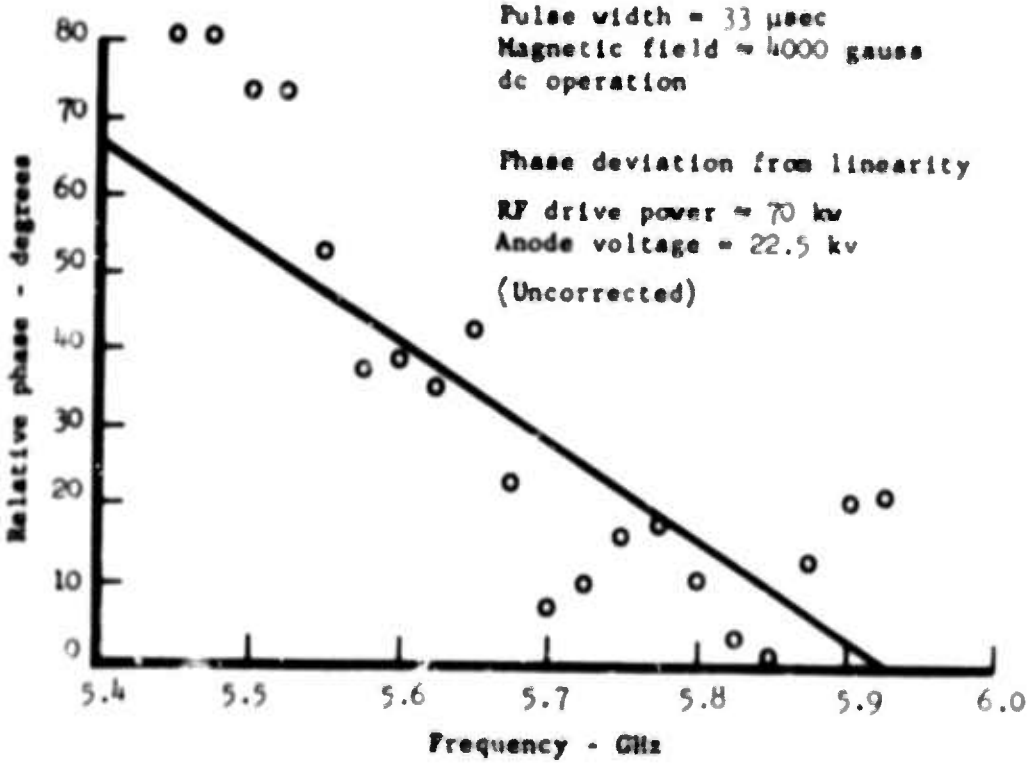

FIGURE 22 PHASE CHARACTERISTICS AS A FUNCTION OF FREQUENCY FOR TUBE J35H

Tube 0.5H-4 was the first vehicle tested. It was operated on the dc test set and peak powers of 300 kv to 350 kv at a duty cycle of 0.001 were obtained. This corresponds to an average power of 2.0 kv to 2.5 kv; the pulse length was 21.5 μsec.

At these power levels, the phase sensitivity to voltage was measured and is shown in Figure 23. The sensitivity is frequency dependent, but is less than 1.5° for a 1% change in voltage at any frequency.

An attempt was made to test the vehicle at higher peak power levels and operation was found to be unsatisfactory. It was felt that the vehicle may have suffered internal damage and was subsequently opened. Upon opening, it was observed that the cathode was not centered and the anode had been slightly damaged.

Due to the time allotted to obtain the information requested by RADC, it was decided not to make any more changes to further develop the vehicle, but to return to the design of the most successful attempt to date, namely J35H. From the previous information obtained on J35H, we decided to rebuild I32H to resemble J35H. The rebuilt I32H was then similar to J35H in all respects except for a minor change in the control electrode geometry. The results obtained were presented at the program review meeting of 1 December 1966.

The vehicle was dc operated across most of the required band at peak power levels of 700 kv to 850 kv at a duty cycle of 0.003. Because of the time allotted and the number of vehicles on hand, it was decided to limit the duty cycle to an area in which it was felt the tube had no chance of being damaged. The results are shown in Figure 24. Saturation curves for the vehicle are shown in Figure 25. The line joining the curves at the 15 kv to 20 kv level indicates the minimum drive level that should be used to avoid a high level of spurious output.

The control electrode V-I characteristics are shown in Figure 26 for two levels of peak operating current. These V-I characteristics are calculated from the measured values by subtracting the component of

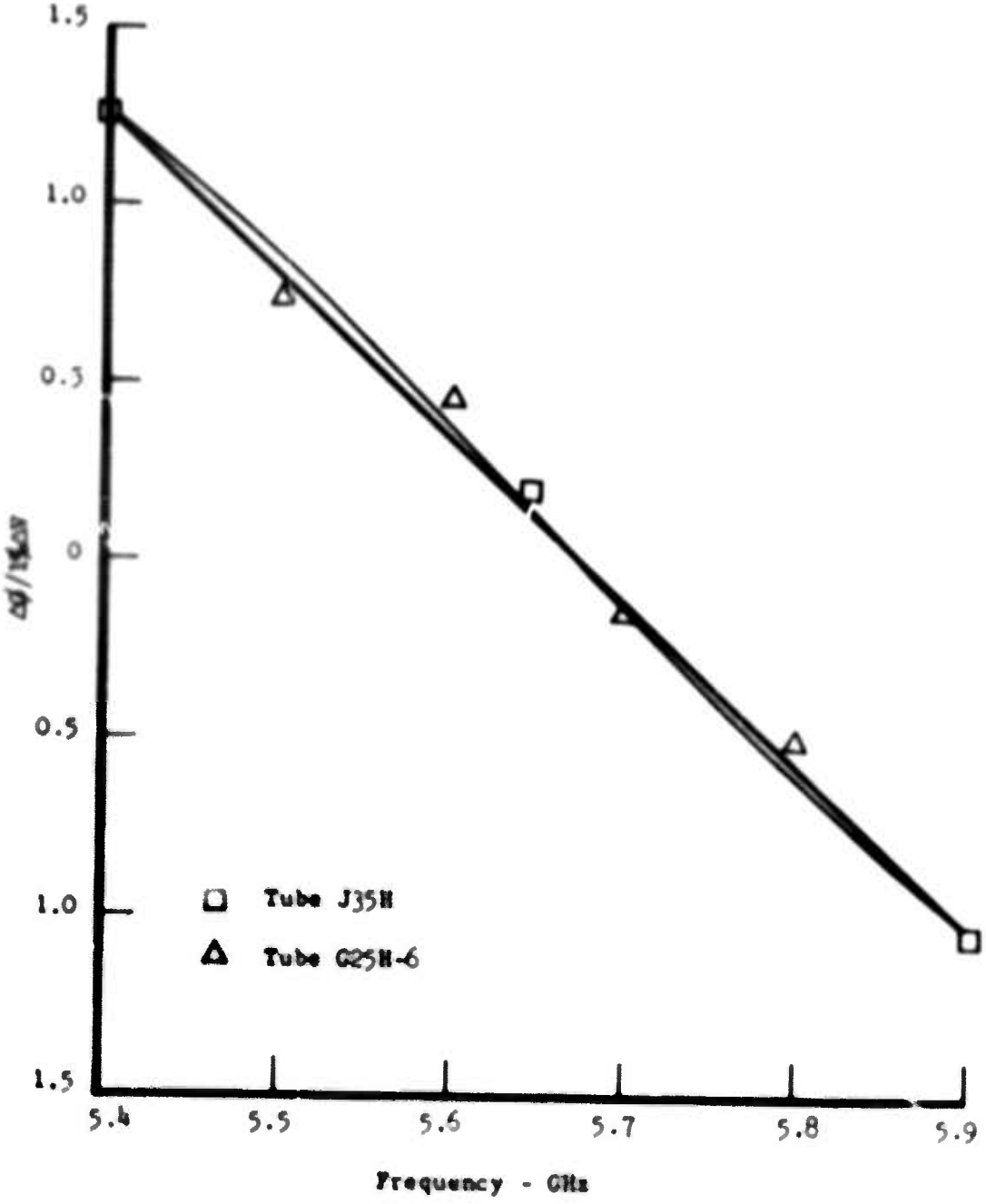

FIGURE 23 PHASE SENSITIVITY TO VOLTAGE AS A FUNCTION OF FREQUENCY

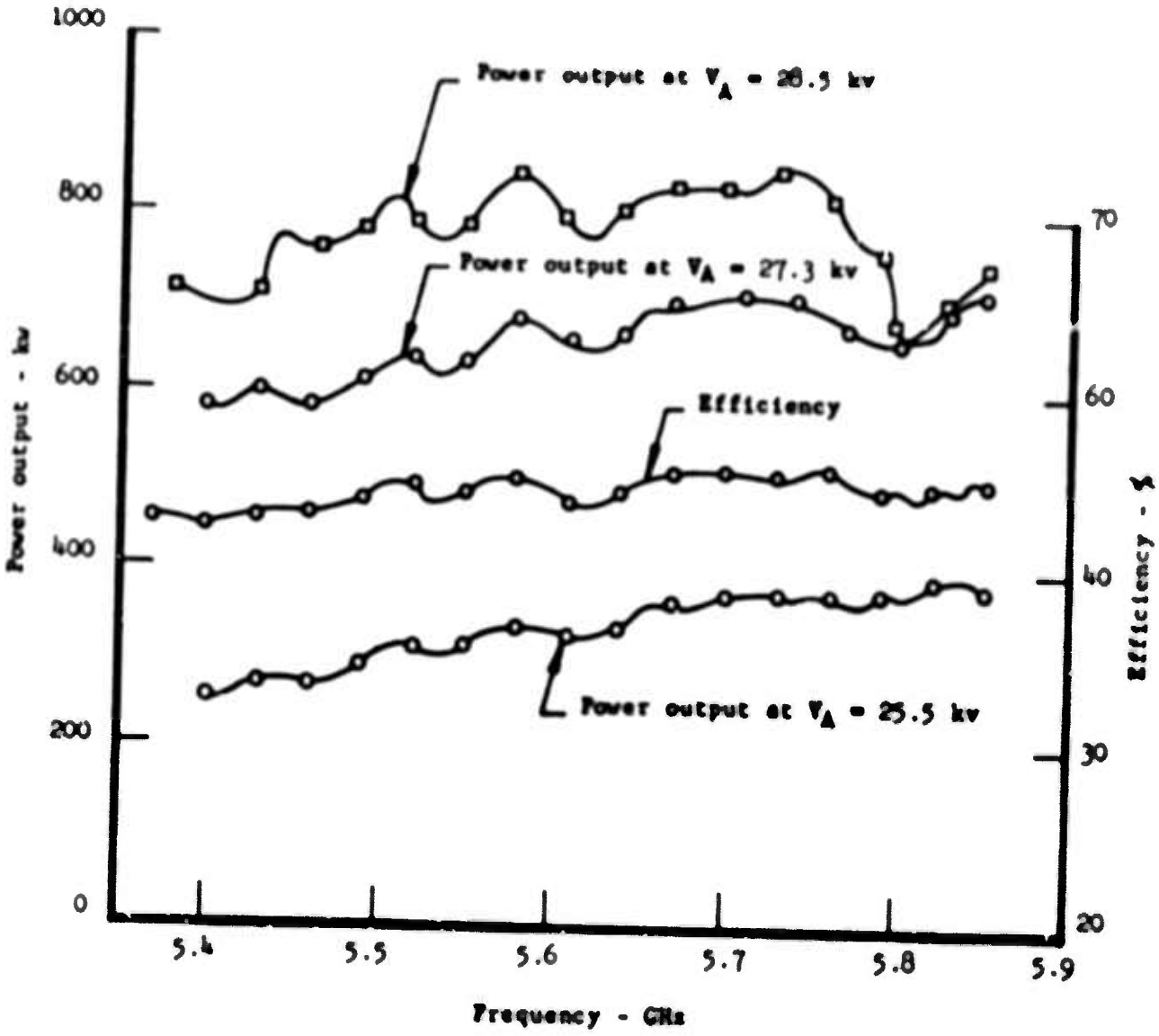

FIGURE 24 POWER OUTPUT VERSUS FREQUENCY FOR TUBE I32H-2

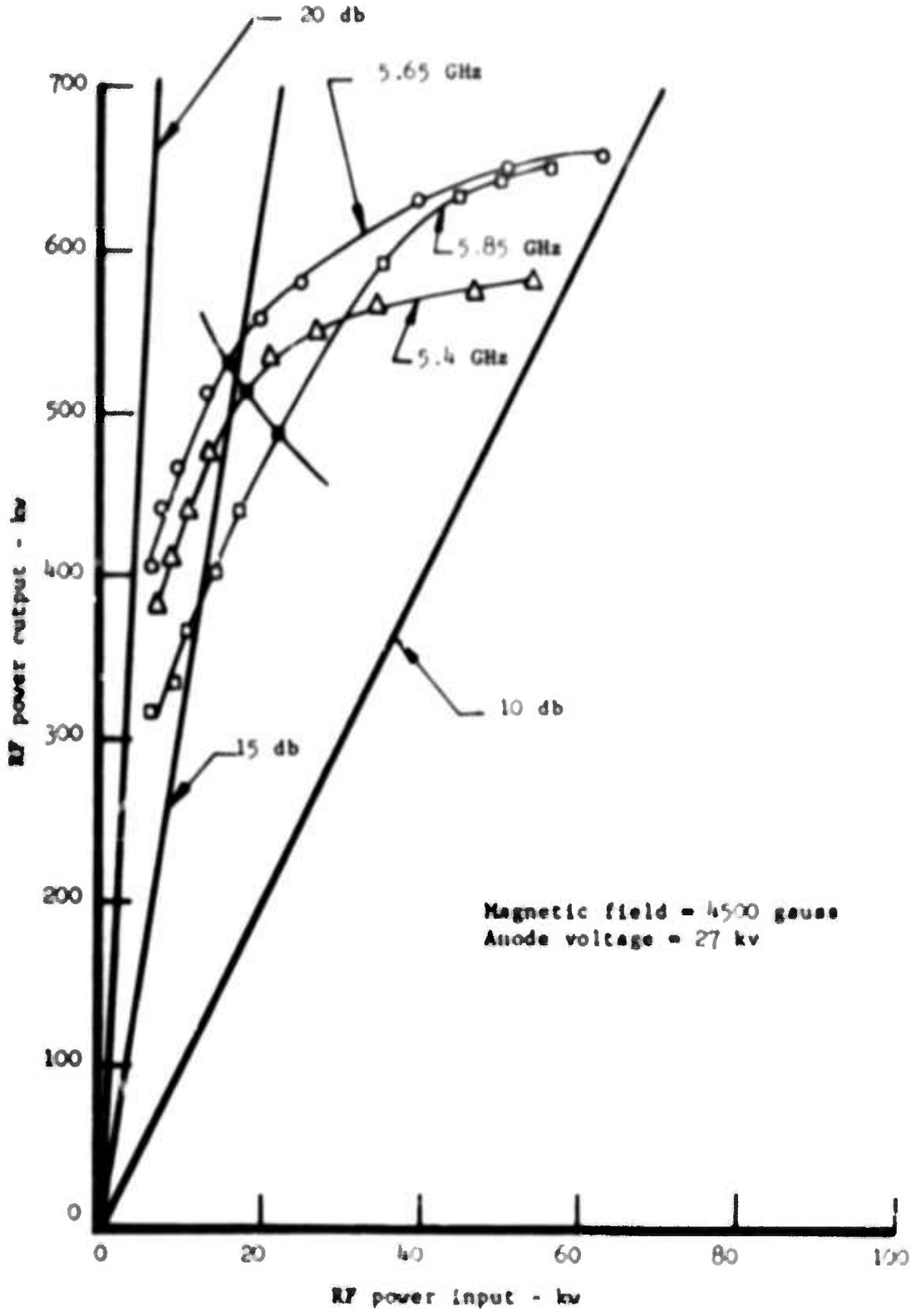

FIGURE 25 POWER OUTPUT VERSUS POWER INPUT FOR TUBE 132H-2

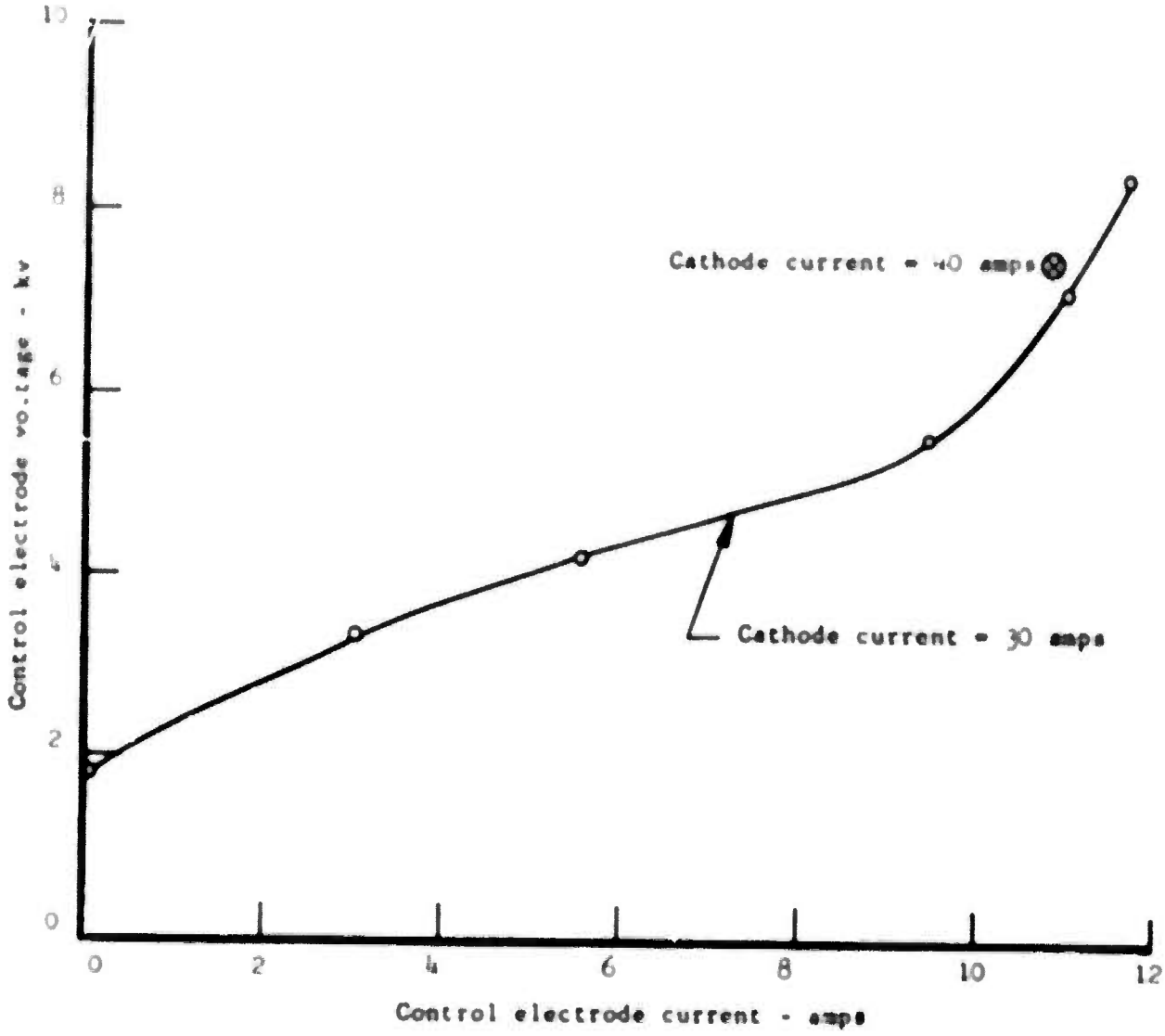

FIGURE 26 V-I CHARACTERISTICS FOR CONTROL ELECTRODE OF TUBE I32H-2

current which charges the interelectrode capacitance from the total measured current. This current is subtracted because it varies with the rate of rise of applied control electrode voltage, while the turn off current is independent of the rate of rise of voltage and the tube operating current. The data indicate that 8.3 kv peak voltage at 11.7 amps peak current are required to turn off the amplifier.

On 8 December 1966, J35M-1 was completed and tested. Initial operation yielded power outputs in the order of 800 kw and operating currents in the order of 80 amps. However, at these levels a tube arc caused immediate degradation of performance and the tube had to be re-aged. After a number of such arcs it became more and more difficult to maintain the higher power levels.

Based on the performance and subsequent degradation of J35M-1, it was decided to make a thorough check of the dc power supply circuitry. Since the failure of J35M-1 was apparently catastrophic, it was felt that the fault energy diverter might not be operating properly. An analysis of the circuit did indeed show that even though the "crow bar" spark gap could be heard to fire, it was not diverting the stored energy. It had been necessary to add additional capacity to the energy storage system external to the dc power supply to reduce the pulse voltage droop. Due to the particular way in which this extra capacity had been added, it was determined that the amplifier fault impedance was much lower than that of the crow bar circuit as seen by the extra capacitance. The net result was that as much as 1000 joules of energy were dissipated in the test vehicle during an arc which could cause the catastrophic failures observed.

It was felt that this condition must be corrected before attempting to operate tube I32M-3 Considerable effort went into rearranging the power supplies and circuitry to insure proper crow bar action. The circuit was tested by using an external spark gap as a fault to test the effectiveness of the crow bar.

Previously, a tube would dissipate as much as 1000 joules of energy during an arc, whereas now it would see less than 1 joule. The effort expended to obtain this operation has been worthwhile as shown by the results obtained on tube 1348-3. At no time did the tube show degradation after an arc as had previously happened.

This tube has been operated at peak power output levels of 1 Mw and higher at pulse lengths of 23 μsec across a 250 MHz band; i.e., from 5.65 GHz to 5.90 GHz the average power levels achieved simultaneously ranged from 5.0 kw to 5.5 kw. The average efficiency observed was 50%. At the upper end of the band, the tube generated 1.2 Mw of peak power and 6.0 kw of average power output at an efficiency of 51.5%.

The tube has also been operated at 600 kw to 900 kw peak power output across the 5.48 GHz to 5.90 GHz band at an average power output of 3.0 kw to 4.5 kw with efficiencies of 45% to 50%, and across a 5.6 GHz to 5.9 GHz band with peak power levels of 880 kw to 1100 kw and an average power level of 4.4 kw to 5.5 kw. This is shown in Figure 27. The pulse length was 23.5 μsec and efficiency was in excess of 45%. For this power level at frequencies below 5.6 GHz, the tube arced after the control electrode extinguished the pulse. Upon investigation it was discovered that the magnetron driver was generating power at frequencies other than the main signal. These frequencies are attributed to the slowly rising and falling characteristic of the magnetron voltage pulse. These modes of operation occur at lower voltages and hence appear before and after the main signal. At frequencies below 5.6 GHz, these spurious outputs were as long or longer than the control electrode pulse and caused the amplifier to restart and to operate continuously, which initiated the arcing. Filters were added to the waveguide system to prevent these spurious outputs from reaching the amplifier input.

At the 6 kw average power level and with the tube operating voltage of approximately 25 kv, the interim dc power supply was at its upper limit.

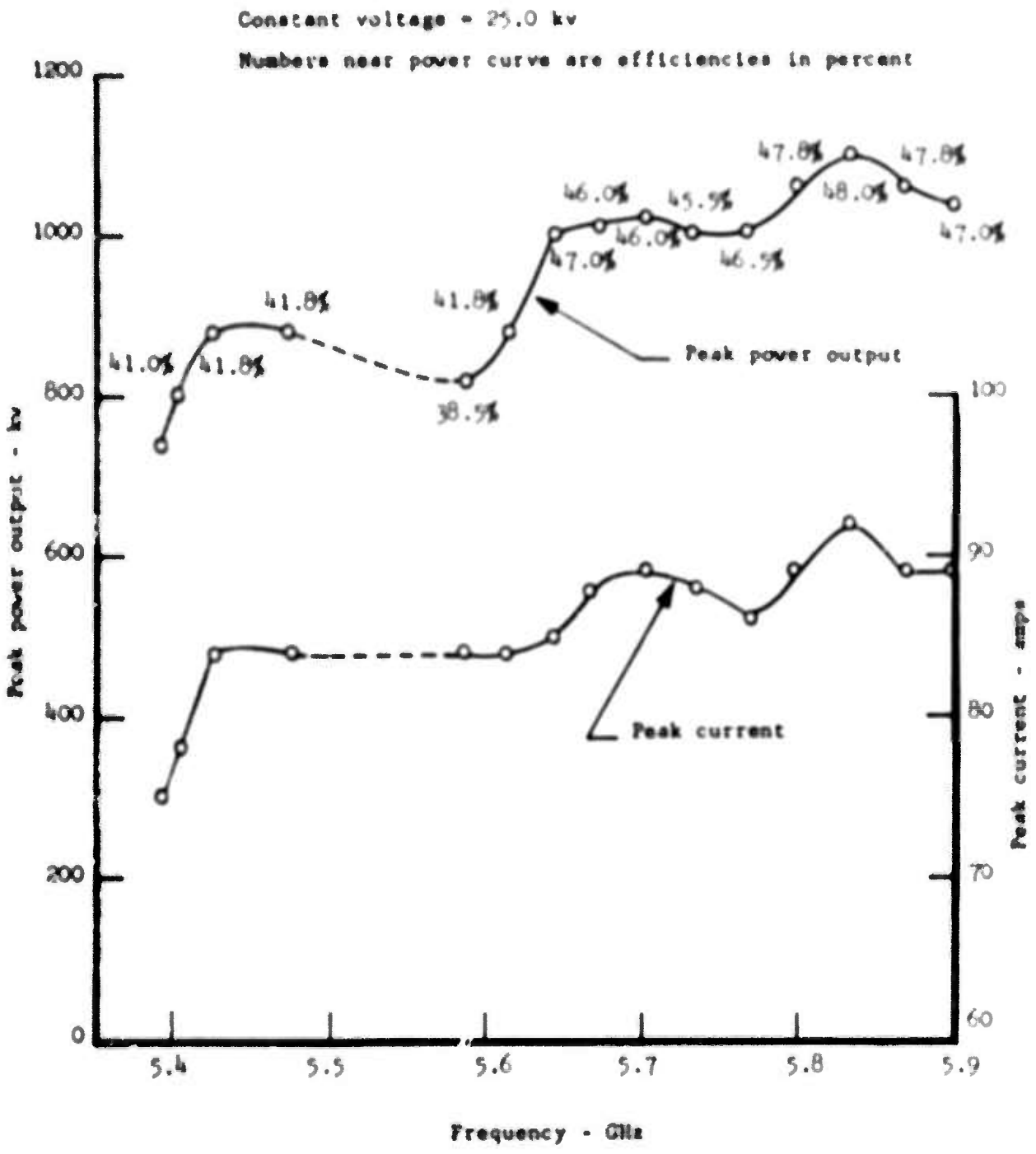

FIGURE 27 PERFORMANCE OF TUBE 1328-3

With the new dc power supply installed and evaluated, tube I32H-3 was again operated. The tube operated at a peak power level of 1 Mw and an average power level of 10 kw. The pulse length was 23.5 usec and the efficiency was in excess of 45%. Before bandwidth data could be taken, the tube underwent a sudden change and could not be operated above a peak power level of 300 kw. It was decided to open the tube. Upon investigation it was noted that the cathode had moved off center. The effect was not related to the power level of operation. The circuit had not been damaged and it was decided to rebuild the tube with the cathode held more firmly in place.

While I32H was being investigated, tube J35H-2 was placed on hot test. The tube had been operated at peak power levels of only 200 kw to 300 kw when a high background pressure was noted. The Vacion® pump operation was suspected and it was decided to replace the pump and to rebake the tube. While the tube was on the exhaust station and at a temperature of 400°C, the tube developed a leak. The leak was discovered in the cathode assembly. The circuit was not damaged and it was decided to rebuild the tube with a new cathode.

Tube No. I32H-4 was delivered to hot test. While on hot test only a short while the tube developed a leak. The tube was opened and since the circuit had not been damaged, the tube was rebuilt. The rebuilding consisted of replacing and modifying a member of the input assembly which had weakened. The remainder of the assembly seemed tight and required no additional work. After the tube was baked, it was returned to the hot test area where the background pressure seemed abnormally high. The tube was leak checked and a small leak was discovered in a ceramic-to-metal seal in the input assembly. In order to evaluate the tube without losing further time in rebuilding, the leak was sealed with glyptol and the tube was rebaked. The tube was returned to hot test where after a short time the leak reappeared.

Tube J35H-3 was now available and it was decided to evaluate this tube rather than to continue working with I32H-5. The tube was

aged and stabilized at a peak power output of 200 kv to 300 kv, although as much as 400 kv to 500 kv were noted during initial aging. Further aging failed to bring the tube to a higher level. It was decided to package the tube with permanent magnets to compare permanent magnet operation with electromagnet operation. Results showed that there was sufficient magnet field for operation.

The final design tube, G15I, was now ready for test. The tube was aged and stabilized in the 200 kv to 300 kv peak power output level and exhibited properties similar to J35M-3. The limited operation prompted an investigation into the possible differences between these particular tubes and tube I32M-3 which generated 1 Mv peak power output at full duty. The investigation showed that the cathode-anode concentricity was as much as 10% different. It was decided to try to place the cathode in a position similar to that of I32M-3 by applying an external force to the cathode. This was first attempt on J32M-3, which was the least dissimilar to I32M-3. The tube not only realized the 400 kv to 500 kv previously noted during the aging process, but approached the 600 kv level.

With this success in mind it was decided to perform the operation on G15I. Although improvement was noted, it was not as significant as that noted with J35M-3. This was due to the fact that G15I was more dissimilar to I32M-3, and with the limited movement available, further improvement could not be obtained.

It was decided to package the tube with permanent magnets to prove the packaging techniques. The tube is now operating in the final package at levels similar to that prior to packaging.

The data are shown in Table I and graphically in Figure 28. Photographs showing the shielded package with external connections and the internal structure with magnetizing coils in place are shown in Figures 29 and 30.

TABLE I

PERFORMANCE DATA FOR SFD-237 IN MAGNETICALLY SHIELDED PACKAGE

Serial No. G151

Operating Conditions: RF input power = 15 kw Control voltage = -8 kv
Pulse length = 21 μsec Coolant flow = 2 gpm
Duty cycle = 0.006

Anode voltage	21 kv		22.3 kv	
Frequency GHz	Current amps	Power output kw	Current amps	Power output kw
5.375	19.2	140	28.4	217
5.400	19.0	140	27.4	217
5.425	19.3	153	28.4	233
5.450	20.5	170	30.0	254
5.475	21.5	180	31.1	273
5.500	22.2	186	30.8	277
5.525	22.0	190	30.0	273
5.550	22.2	193	29.5	270
5.575	22.5	200	30.5	270
5.600	22.5	196	30.3	273
5.625	22.2	200	30.0	270
5.650	22.9	200	29.2	273
5.675	23.3	203	30.0	382
5.700	22.9	183	29.5	250
5.725	23.4	190		
5.750	24.2	206		
5.775	23.3	190		
5.800	22.9	193		
5.825	24.5	210		
5.850	23.3	200		
5.875	23.9	200		
5.900	23.3	200		
5.925	21.3	180		
5.950	22.2	190		
5.975	22.0	183		

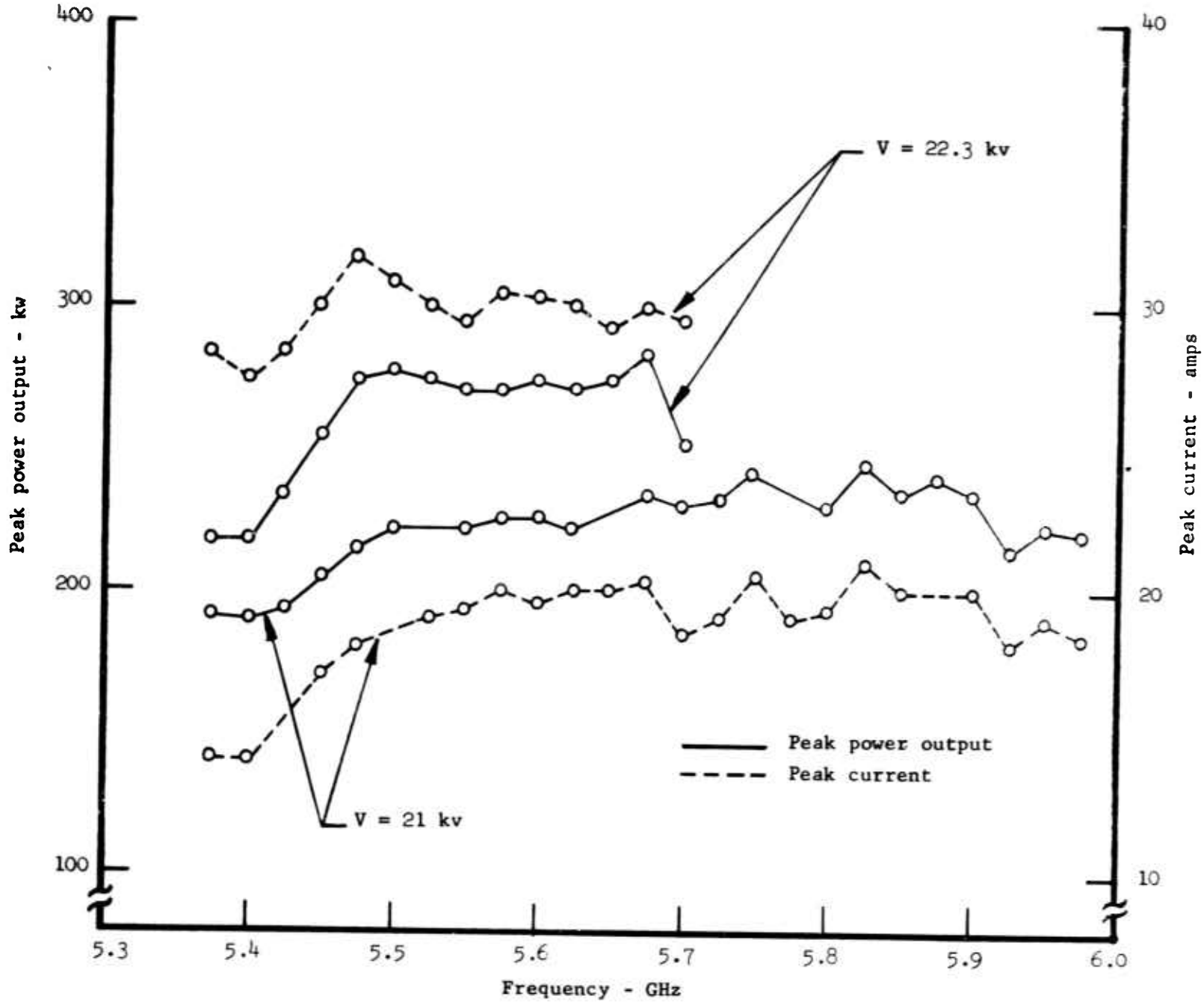

FIGURE 28 PERFORMANCE DATA FOR SFD-237, TUBE G15I, IN MAGNETICALLY SHIELDED PACKAGE

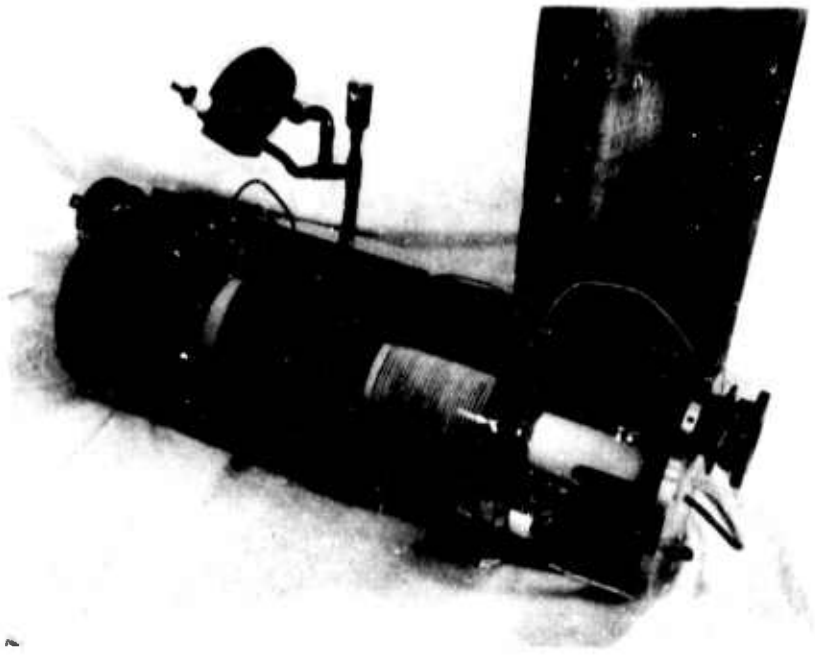

FIGURE 29 PHOTOGRAPH OF MAGNETICALLY SHIELDED PACKAGE, INTERNAL VIEW

FIGURE 30 PHOTOGRAPH OF TUBE G15I, MAGNETICALLY SHIELDED PACKAGE

5.0 CONCLUSIONS

The tube developed during this program is a pulsed crossed-field amplifier which operates from a dc voltage supply through cold cathode operation with RF turn on and control electrode turn off. The amplifier operation has been demonstrated at peak power output levels of 1 Mw and higher at pulse lengths of 23·μsec across a 250 MHz band from 5.65 GHz to 5.9 GHz. The average power achieved simultaneously ranged from 5.0 kw to 5.5 kw. The average efficiency observed was 50% and the operating voltage was approximately 25 kv. At the upper end of the band, the amplifier was operated at 1 Mw peak power and 10 kw of average power. The amplifier was also demonstrated with a 600 kw to 900 kw peak power output across 5.48 GHz to 5.9 GHz.

The phase performance of the amplifier was also demonstrated to have the following characteristics: phase sensitivity to voltage was approximately 1° per 1% change in voltage across most of the band; phase sensitivity to RF drive power varied from approximately 6° per 1 db change at the low frequency end of the band to less than 1° per 1 db change at the high end of the band. The phase deviation from linearity was demonstrated to be approximately 20° peak to peak with the tube operating at the 700 kw to 850 kw level with the RF input at 50 kw. The deviation from linearity was found to be periodic and related to a feedback mechanism in the tube. The cold, that is non-operating phase deviation was found to be approximately 10° peak to peak with the same periodicity as in the operating amplifier. It was therefore concluded that the feedback results from insufficient decoupling of the RF power between the input and output sections of the slow wave circuits.

In general, most of the target specifications have been achieved and demonstrated but not necessarily at the same time.

A magnetically shielded packaged amplifier with integral magnets was constructed and delivered. The package has a 10 inch

diameter and is 32 inches long. The input and output waveguides are arranged parallel to the axis of the amplifier and are located at the ends of the package. The coolant input and output and the high voltage connections are located on the input end of the package.

The performance of the packaged amplifier fell short of the target specifications. Operation was limited to 200 kw to 300 kw peak power output at reduced voltage. The reduced performance was due to a severe anode-cathode eccentricity which could not be corrected with the remaining funds and time.

6.0 RECOMMENDATIONS

The SFD-237, in its present state, very nearly meets the minimum specifications. However, it appears to be quite possible to extend the operation to meet the full target specifications of 1 Mw peak power output across the full 500 MHz band. In order to accomplish this, it would be necessary to alter the dispersion characteristics so that the tube would operate at a higher range of phase shift per section. To alter the phase shift range, a slight adjustment of the anode slow wave circuit will be necessary. No further major change is deemed necessary since the vehicles have demonstrated their average power capability.

A very interesting area of future study is the possibility of introducing "self-turn off"; that is, to have the amplifier cease current conduction when the RF drive power is removed. Removal or reduction of the control electrode turn off would considerably simplify modulator requirements.

A third area of study should be experiments to determine the operating life of this type of vehicle at high peak and average powers with relatively high peak and average cathode current. Very little is known of the operating life of cathode materials in this operating range.

APPENDIX

TEST PROCEDURE

SFD-237

1.0 PURPOSE AND SCOPE

The purpose of this document is to specify the test procedures to be used in demonstrating the conformance of the SFD-237 to the specifications of Exhibit "A" (as modified) of Contract AF 30(602)-4082. The specifications are included.

2.0 STANDBY MECHANICAL TEST

The static water pressure test shall be performed on the coolant chambers by applying water at 45 spig minimum. No leaks shall occur in the coolant chamber fittings. The time of the test shall be at least one (1) minute.

3.0 OPERATIONAL TESTS

3.1 Pre-test Conditions

The following conditions shall be set before starting the test.

3.1.1 The coolant flow rate shall be set at 2.5 ± 0.1 gpm.

3.1.2 The calorimeter flow rate shall be noted and recorded on the Acceptance Test Data Sheet (ATDS).

3.1.3 The calorimeter thermometer readings shall be noted for the initial Δt after a sufficient time has elapsed to allow for thermal equilibrium. The initial Δt shall be recorded on the ATDS.

3.2 Test Conditions (Minimum Acceptance Conditions)

3.2.1 The RF pulse length shall be set at 19-21 μsec measured at the 3 db points on the RF pulse envelope. The repetition frequency shall be set for a maximum duty cycle of 0.01.

3.2.2 The RF input power shall be set to 70 kw peak maximum at the input to the crossed-field amplifier (CFA) at all test frequencies. The RF input power shall be monitored by suitable means to insure proper drive power at all test frequencies.

3.2.3 The control electrode voltage pulse shall be set at 8.3 kv maximum. The pulse shall be positioned so that it begins at the point where the RF input pulse power drops approximately 1 db below the average peak value. The control voltage shall be maintained until the RF drive power is completely removed.

3.2.4 With the drive turned off and with the control electrode voltage properly adjusted for time sequence as described above, the dc power supply shall be turned on and set to the specified operating voltage (-25 kv maximum). The RF drive can now be applied. This procedure shall be followed each time the dc voltage is removed from the tube.

3.3 Power Output

With the control electrode voltage properly applied and with the dc voltage set at the specified value, the power output shall be measured as described in Section 4.2. The RF input power at the CFA

input shall not exceed 70 kw and shall be adjusted at each test frequency. The power output shall be measured at 0.01 GHz increments from 5.4 GHz to 5.9 GHz.

The dc voltage setting shall remain fixed at the specified value throughout the test and this voltage shall not exceed -25 kv. The average current shall not be more than 0.700 amps for the 0.01 duty cycle. The average output power shall not be less than 7 kw nor more than 11.1 kw at any test frequency in the band. Each measurement of voltage, current, and power output shall be recorded on the ATDS.

3.4 Efficiency

The efficiency shall be calculated on an average power basis from the results obtained in Section 3.3. The efficiency is defined as the ratio of RF power output to the product of the average current and the dc voltage. The minimum efficiency at any test frequency shall be 40%. The average efficiency shall be 45% minimum. The average efficiency is defined as the sum of the efficiencies obtained at the eleven test points divided by eleven.

3.5 Starting Time Jitter

The starting time jitter shall be measured by observing the pulse to pulse variation of starting time references to the RF input pulse. The leading edge of the envelope of the RF output pulse will be displayed on an oscilloscope which has the time base triggered by the envelope of the RF input pulse. The time base shall be 10 nanoseconds per centimeter. The starting jitter shall not exceed 10 nanoseconds as observed during any 1 second interval. This measurement shall be made with rated power output at a frequency of 5.9 GHz. The measurement data shall be recorded on the ATDS.

3.6 Phase Linearity

3.6.1 The phase linearity shall be measured using the method described in Section 4.3. The measurements shall be made in 0.05 GHz increments from 5.4 GHz to 5.9 GHz with the amplifier operating at rated conditions. The deviation from linearity is defined as the departure from a straight line drawn through the eleven measurement points. The maximum peak to peak deviation shall not exceed TBS degrees.

3.6.2 At the frequencies of 5.4 GHz, 5.65 GHz, and 5.9 GHz a calibrated VSWR shall be interposed between the CFA and the load. The calibrated VSWR shall be the equivalent of a 2.5:1 mismatch as seen through a circulator having at least 20 db isolation between input and output. The circulator input VSWR shall not exceed 1.25:1 when the output is terminated with a mtached load. The phase of the calibrated VSWR shall be adjusted to obtain minimum RF output power at rated voltage at each of the three frequencies. The deviation from the straight line drawn through the three points shall not exceed plus or minus TBS degrees.

3.7 Spurious Power Output

The spurious power output shall be measured by the method shown in Section 4.4.

3.7.1 The spurious power output with the beam on shall be at least 35 db below the signal amplitude when both signal and noise are measured using a 3 MHz bandwidth filter. Spurious power output shall be checked from 5.3 GHz to 6.0 GHz excluding a band plus or minus 10 MHz around the center of the signal spectrum. The measurements shall be made at 5.4 GHz, 5.65 GHz, and 5.9 GHz and recorded on the ATDS.

3.7.2 The spurious power output with the beam off will be measured using the method described in Section 4.5. This test shall be conducted only after completion of all tests mentioned above. The spurious power output with the beam off shall not exceed -104 dbm/MHz over the operating band between 5.4 GHz and 5.9 GHz.

3.8 Phase Tracking

The phase tracking characteristics shall be measured using the method described in Section 4.3 and compared with a suitable standard.

4.0 MEASUREMENT TECHNIQUES FOR ACCEPTANCE TEST PROCEDURES

All electrical test equipment pertinent to the measurements indicated below are calibrated in the S-F-D laboratories' Calibration Control Program.

4.1 Tube Operating Parameters

4.1.1 Voltage

The voltage will be measured with a Sensitive Research Instrument Co. electrostatic voltmeter, Model Eshpot.

4.1.2 Average Current

The average current will be measured with a Weston dc milliammeter, Model 1761, or equivalent.

4.1.3 Frequency

The frequency will be measured with a Hewlett-Packard frequency meter, Model J532A.

4.1.4 Duty Cycle

The duty cycle will be measured using a Tektronix oscilloscope, Model 543A with a type CA plug in unit.

4.1.5 RF Power

The RF power will be measured with a calorimeter (as explained under Section 4.1.6, Power Output) and/or by a Hewlett-Packard microwave power meter, Model 430C, in conjunction with calibrated directional couplers.

4.1.6 Power Output

The power output of the tube will be measured on an average power basis using a water load and calorimeter, as shown in Figure 1. The VSWR of the water load will be measured across the frequency band and shall be less than 1.10:1.

The calorimeter flow rate is adjustable up to at least 2000 cc/min and the thermometers are marked in divisions of 0.1°, yielding

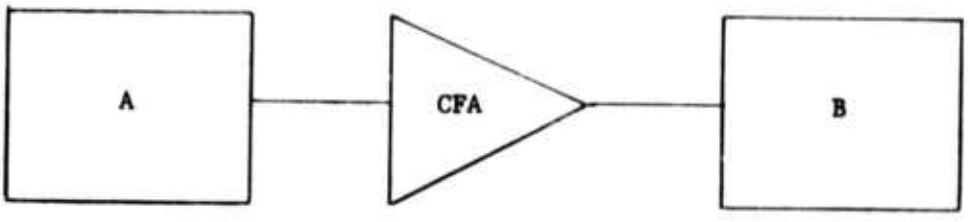

A Modified SFD-313 magnetron

B Bogart C-band water load

FIGURE 1 TEST SET FOR MEASURING POWER OUTPUT

a resolution of about 0.05°. (At a 1000 cc/min flow rate, a 0.1° temperature difference corresponds to less than 7 watts of average power. Thus at the rated average power, the resolution error is less than 0.1%.)

The calorimeter will be calibrated using a substitution method. A water-cooled resistance will be placed in series with the water load. With the flow rate at 1000 cc/min and the inlet water set at a reference temperature, a known amount of (60 Hz) power will be applied to the resistance. (This power will be measured using a standard calibrated wattmeter.) The power will then be calculated from the temperature rise of the thermometer and a calibration curve for the calorimeter will be made. All measurements are made when the system reaches equilibrium conditions (approximately 3 minutes after making any change).

An accuracy of plus or minus 3% is anticipated.

4.2 Phase Measurements

The technique to be used is a modified version of a null detection method as shown in schematic form in Figure 2.

The length of the input arm of the phase bridge is adjusted so that the rate of change of phase with frequency of the output arm is adjusted with the amplifier operating at approximately mid-band. The total linear change in phase with the amplifier operating should not exceed 50° when the amplifier is tuned across the operating band of frequencies.

The measurement to be made is the phase deviation from a straight line so that the measurement begins by balancing the bridge using the precision attenuator (H) and the phase shifter (G) to obtain a deep null as viewed on the oscilloscope (F). This initial balancing may be started at either end of the operating band with the amplifier operating. The measurement proceeds by tuning the frequency across the operating band in approximately ten steps. At each step, the phase shifter (G) is adjusted to bring the display to a null on the oscilloscope (F). The amount of phase change is read directly from the phase

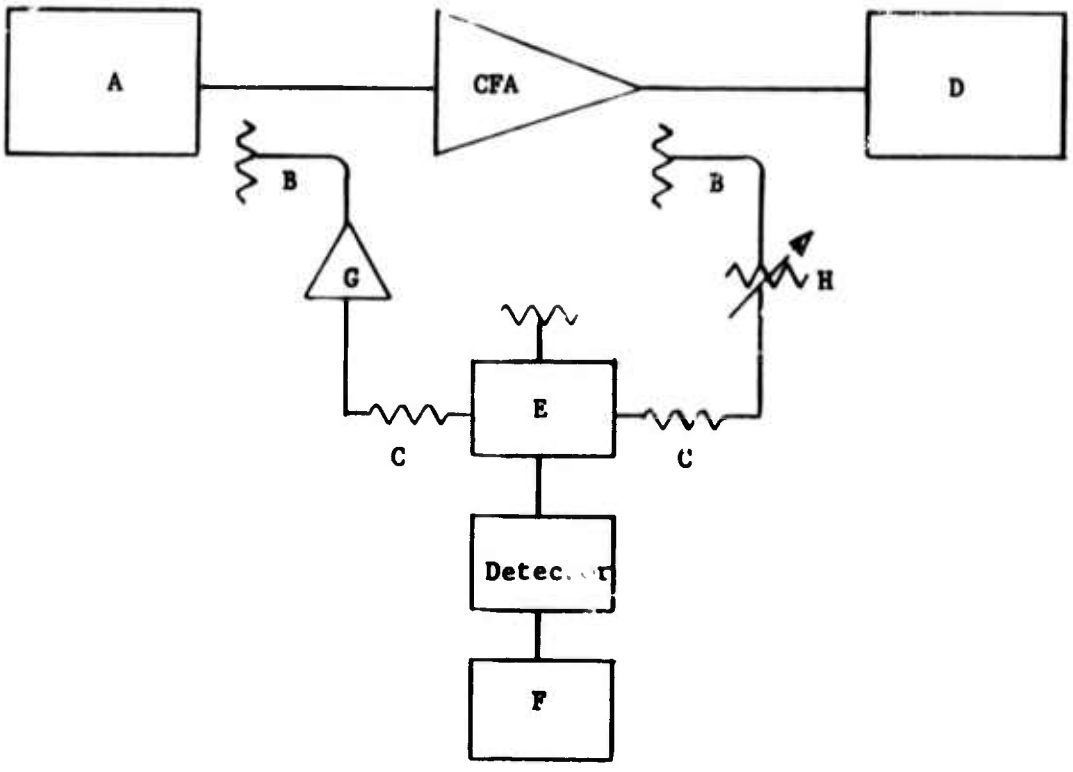

A Modified SFD-313 magnetron

B Narda Model 1083 directional coupler

C Hewlett Packard attenuator Model J372D

D Bogart C-band water load

E Hybrid T

F Tektronix plug in amplifier

G Hewlett Packard phase shifter Model J885A

H Hewlett Packard precision attenuator Model J382A

FIGURE 2 PHASE MEASUREMENT TEST SET

shifter (G). The precision attenuator need not be changed after the initial adjustment since the amplitude of the signal in both arms will remain essentially constant. The eleven points so obtained are plotted as a change of phase as a function of frequency, and a straight line is drawn through the points. The deviation from linearity is measured as the distance between the line and the recorded point.

The components of the phase bridge are especially selected for this type of measurement (high directivity directional couplers, low VSWR attenuators, etc.) so that measurement errors (particularly errors due to reflections from system components) will not be a major problem. The system should have a plus or minus 1^{o} accuracy.

4.3 Noise Measurements

The block diagram of the noise measurement test set is shown in Figure 3. In this set up, a portion of the amplifier signal is mixed with a local oscillator to obtain a 30 MHz output. The local oscillator is a linearly swept backward wave oscillator (BWO) whose frequency range is 4 GHz to 8 GHz. The output of the mixer is fed through a 3 MHz band pass filter centered at 30 MHz. This signal is fed through an IF strip. The output is displayed on an oscilloscope. By using a calibrated attenuator in the IF strip, the power output at any frequency can be compared to the power output at the signal frequency. An accuracy of plus or minus 1 db is expected.

To measure the noise with the beam off, the system is calibrated against a calibrated noise source. The output of the CFA with the specified voltage applied is mixed with the swept local oscillator and compared with the noise obtained from the calibrated source.

4.4 Interpulse Noise Measurement

The block diagram of the interpluse noise measurement set is shown in Figure 4.

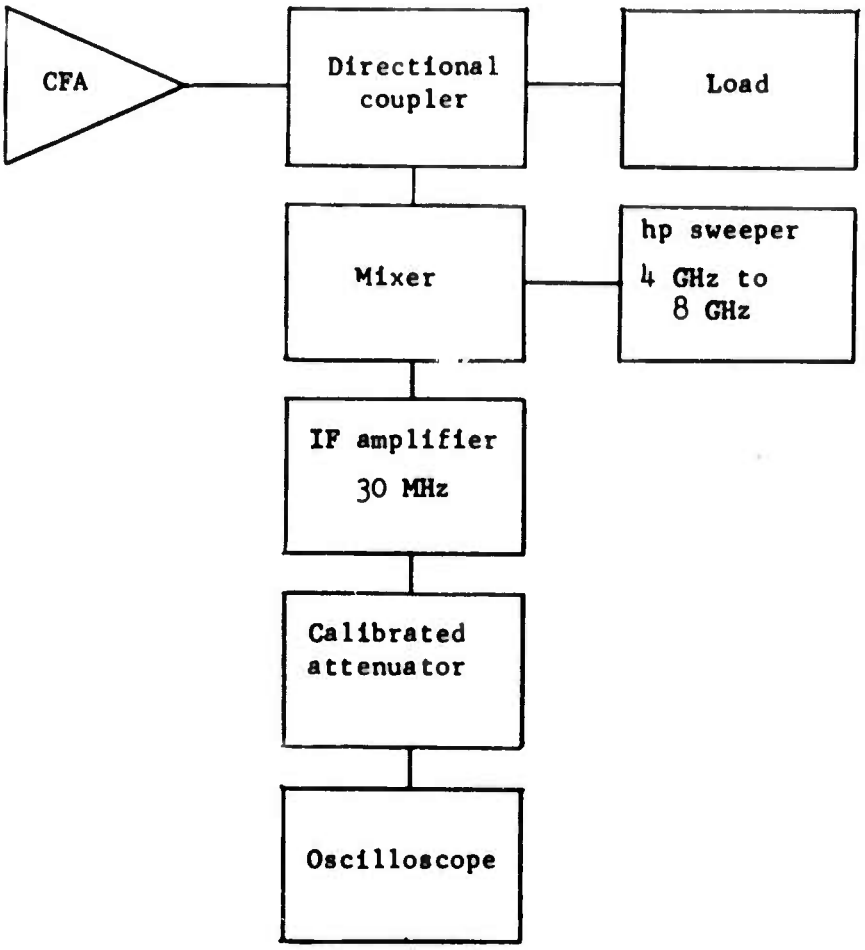

FIGURE 3 NOISE MEASUREMENT TEST SET

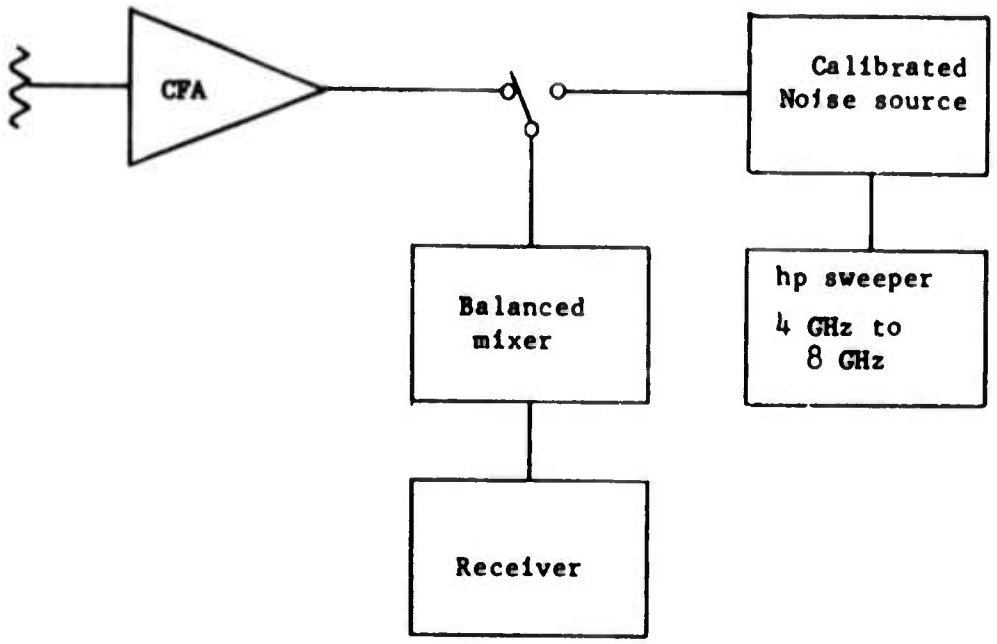

FIGURE 4 INTERPULSE NOISE MEASUREMENT TEST SET

This measurement is to be made by running hot water through the CFA coolant channels so that the temperature of the CFA can be raised to somw value above the ambient temperature. The RF input port to the CFA is to be terminated in a matched load and a dc voltage is applied to the cathode. The RF output port is coupled to a balanced mixer. A calibrated noise source is provided to calibrate the entire noise detection system. The interpulse noise output of the CFA is then compared against the calibrated source across the operating frequency band.

SFD-237 PERFORMANCE SPECIFICATIONS

Center frequency	5.65 GHz
Instantaneous bandwidth	Min: 2 db Target: 1 db Goal: 0.25 db } 500 MHz (with constant voltage and constant drive
Peak power output	Min: 700 kw Target: 1 Mw Goal: 2 Mw
Average power output	Min: 7 kw Target: 10 kw Goal: 20 kw
Gain	Min: 10 db Target: 13 db Goal: 15 db
Cathode voltage	-25 kv maximum
Control electrode mu	3 minimum
Efficiency	
Minimum	40%
Average	Min: 45% Target: 50% Goal: 55%
Phase linearity	plus or minus 2.5 degrees maximum from linear across the 500 MHz bandwidth (objective)
Phase tracking	plus or minus 5.0 degrees maximum across the 500 MHz bandwidth between any two of any number of amplifiers operated in parallel under identical dc and frequency conditions (objective)
Pulse width	Shall be capable of the following: Min: 20 µsec Target: 50 µsec Goal: 60 µsec

Load VSWR capability	When operated with a circulator, a mismatch of up to 2.5:1 at any phase angle shall not alter any other parameter outside of the specification limit
Starting time jitter	Shall not exceed 10 nanoseconds, with 5 nanoseconds as an objective
Noise	-104 dbm/MHz maximum contributed by the tube during the interpulse period and -35 db during the pulse (3 MHz integrated)
Cooling	Water cooling shall be employed with one input and one output connection to the package at ground potential
Magnetic field	Permanent magnets shall be employed
Package	Maximum transverse dimension is 9 inches. Package shall be magnetically shielded
Demonstration	The contractor shall demonstrate, at the contractor's plant, that the tube(s) operate in accordance with the specification stated herein. The demonstration shall be conducted in accordance with the approved test procedures.

Unclassified
Security Classification

DOCUMENT CONTROL DATA - R & D

(Security classification of title, body of abstract and indexing annotation must be entered when the overall report is classified)

1. ORIGINATING ACTIVITY (Corporate author)
S-F-D laboratories, inc.
800 Rahway Avenue
Union, New Jersey

2a. REPORT SECURITY CLASSIFICATION
Unclassified

2b. GROUP
---

3. REPORT TITLE
DEVELOPMENT OF A C-BAND PHASED ARRAY CROSSED-FIELD AMPLIFIER

4. DESCRIPTIVE NOTES (Type of report and inclusive dates)
Final Report

5. AUTHOR(S) (First name, middle initial, last name)
A. Wilczek

6. REPORT DATE	7a. TOTAL NO. OF PAGES	7b. NO. OF REFS
January 1968	73	--

8a. CONTRACT OR GRANT NO.	9a. ORIGINATOR'S REPORT NUMBER(S)
AF 30(602)-4082	78-F
b. PROJECT NO.	
c. ARPA Order No. 136 Amendment No. 11	9b. OTHER REPORT NO(S) (Any other numbers that may be assigned this report) RADC-TR-68-170
d.	

10. DISTRIBUTION STATEMENT This document is subject to special export controls and each transmittal to foreign governments, foreign nationals or representatives thereto may be made only with prior approval of RADC (EMATE), GAFB, N.Y.

11. SUPPLEMENTARY NOTES	12. SPONSORING MILITARY ACTIVITY
	Advanced Research Projects Agency/ Rome Air Development Center, AFSC Griffiss Air Force Base, New York

13. ABSTRACT

A C-band phased array crossed-field amplifier, capable of delivering 1 Mw peak power with 10 kw average power output over a 500 MHz band centered at 5.65 GHz, has been developed. This tube is dc operated with control electrode turn off and is packaged in a 10 inch diameter magnetically shielded package with integral permanent magnets.

This tube employs a new slow wave structure developed under an earlier program. Matching studies on this circuit, the helix coupled vane (HCV) circuit, have resulted in a good match over approximately 1 GHz.

A cathode material study evaluated several materials for use in the high power dc operated amplifier. An impregnated tungsten matrix type cathode was used on the program as a result of this study.

Peak power levels of 700 kw to 805 kw at a pulse length of approximately 32 μsec with nearly full instantaneous bandwidth resulted from dc operation of a vehicle in an electromagnet. This tube subsequently operated at 5.9 GHz and generated 1 Mw peak power output with 10 kw of average power output.

Phase measurements were performed on three vehicles.

DD FORM 1 NOV 68 1473

Unclassified
Security Classification